Cardiac Hypertrophy Is Inhibited by a Local Pool of cAMP Regulated by Phosphodiesterase 2

Anna Zoccarato, Nicoletta C. Surdo, Jan M. Aronsen, Laura A. Fields, Luisa Mancuso, Giuliano Dodoni, Alessandra Stangherlin, Craig Livie, He Jiang, Yuan Yan Sin, Frank Gesellchen, Anna Terrin, George S. Baillie, Stuart A. Nicklin, Delyth Graham, Nicolas Szabo-Fresnais, Judith Krall, Fabrice Vandeput, Matthew Movsesian, Leonardo Furlan, Veronica Corsetti, Graham Hamilton, Konstantinos Lefkimmiatis, Ivar Sjaastad, Manuela Zaccolo

Rationale: **Chronic elevation of 3′-5′-cyclic adenosine monophosphate (cAMP) levels has been associated with cardiac remodeling and cardiac hypertrophy. However, enhancement of particular aspects of cAMP/protein kinase A signaling seems to be beneficial for the failing heart. cAMP is a pleiotropic second messenger with the ability to generate multiple functional outcomes in response to different extracellular stimuli with strict fidelity, a feature that relies on the spatial segregation of the cAMP pathway components in signaling microdomains.**

Objective: **How individual cAMP microdomains affect cardiac pathophysiology remains largely to be established. The cAMP-degrading enzymes phosphodiesterases (PDEs) play a key role in shaping local changes in cAMP. Here we investigated the effect of specific inhibition of selected PDEs on cardiac myocyte hypertrophic growth.**

Methods and Results: **Using pharmacological and genetic manipulation of PDE activity, we found that the rise in cAMP resulting from inhibition of PDE3 and PDE4 induces hypertrophy, whereas increasing cAMP levels via PDE2 inhibition is antihypertrophic. By real-time imaging of cAMP levels in intact myocytes and selective displacement of protein kinase A isoforms, we demonstrate that the antihypertrophic effect of PDE2 inhibition involves the generation of a local pool of cAMP and activation of a protein kinase A type II subset, leading to phosphorylation of the nuclear factor of activated T cells.**

Conclusions: **Different cAMP pools have opposing effects on cardiac myocyte cell size. PDE2 emerges as a novel key regulator of cardiac hypertrophy in vitro and in vivo, and its inhibition may have therapeutic applications. (*Circ Res*. 2015;117:707-719. DOI: 10.1161/CIRCRESAHA.114.305892.)**

Key Words: cAMP ■ cyclic nucleotide ■ hypertrophy ■ phosphodiesterases 2 ■ protein kinase A ■ signal transduction

The pleiotropic second messenger 3′-5′-cyclic adenosine monophosphate (cAMP) mediates the catecholaminergic control on heart rate and contractility and, at the same time, is responsible for the functional response of the heart to a wide variety of other hormones and neurotransmitters. cAMP signaling is also central to the pathogenesis of several conditions, including cardiac hypertrophy, arrhythmia, and heart failure.[1] An important advance in cardiac adrenergic signal transduction is the realization in the past decade that the high fidelity with which cAMP mediates a plethora of different functions relies on the spatial segregation of the molecular components of this signaling pathway within subcellular microdomains.[2,3] The hormonal specificity of cAMP action[4] results from the generation of distinct pools of the second messenger, which in turn mediates different functional outcomes via activation of different subsets of the cAMP effector protein kinase A (PKA).[5,6] PKA is a holotetrameric enzyme composed of a dimer of regulatory (R) and 2 catalytic (C) subunits. In the heart,

Original received December 23, 2014; revision received August 2, 2015; accepted August 4, 2015. In July 2015, the average time from submission to first decision for all original research papers submitted to *Circulation Research* was 12.38 days

From the Institute of Neuroscience and Psychology (A.Z., L.A.F., A.S., C.L., H.J., F.G., A.T., G.H., M.Z.) and Institute of Cardiovascular and Medical Sciences (Y.Y.S., G.S.B., S.A.N., D.G.), University of Glasgow, Glasgow, UK; Department of Physiology, Anatomy and Genetics, University of Oxford, Oxford, UK (N.C.S., K.L., M.Z.); Institute for Experimental Medical Research, Oslo University Hospital and University of Oslo, Oslo, Norway (J.M.A., I.S.); Venetian Institute of Molecular Medicine, University of Padova, Padova, Italy (L.M., G.D., A.T., L.F., V.C.); Cardiology Section, VA Salt Lake City Health Care System and Cardiovascular Medicine Division, University of Utah School of Medicine, Salt Lake City, UT (N.S.-F., J.K., F.V., M.M.); Bjorknes College, Oslo, Norway (J.M.A.); and BHF Centre of Research Excellence, Oxford, UK (K.L., M.Z.).

The online-only Data Supplement is available with this article at http://circres.ahajournals.org/lookup/suppl/doi:10.1161/CIRCRESAHA.114.305892/-/DC1.

Correspondence to Dr Manuela Zaccolo, Department of Physiology, Anatomy and Genetics, Sherrington Bldg, Parks Rd, Oxford OX1 3PT, UK. E-mail manuela.zaccolo@dpag.ox.ac.uk

Nonstandard Abbreviations and Acronyms	
AKAP	A kinase anchoring protein
ARVM	adult rat ventricular myocyte
cAMP	3′-5′-cyclic adenosine monophosphate
NFAT	nuclear factor of activated T cells
NRVM	neonatal rat ventricular myocyte
PDE	phosphodiesterase
PKA	protein kinase A
TAC	transverse aorta constriction

2 PKA isoforms are expressed, PKA type I and PKA type II, which differ in their R subunit. In cardiac myocytes, PKA is largely localized to different subcellular compartments[6] via binding to a family of scaffolding proteins known as A kinase anchoring proteins (AKAPs).[7] Apart from their common ability to anchor PKA, AKAPs show a high degree of structural variability, which allows for different subcellular localization and binding to a variety of signaling components. As a result, AKAPs serve as signaling centers, where specific binding partners are organized for a particular task. Localization of PKA is achieved through the interaction of the amino-terminal dimerization/docking domain of the R subunits[8] with the AKAP and serves to anchor PKA in proximity to selected targets, thus favoring their preferential phosphorylation.[9–11] The AKAP-dimerization/docking interaction is also responsible for differential targeting of the 2 PKA isoforms, with different AKAPs showing different specificity of binding for RI and RII[12] as a consequence of differences within the docking interface in R.[13]

The intracellular concentration of cAMP is tightly regulated by the cyclic nucleotide degrading enzymes phosphodiesterases (PDEs). PDEs are a large superfamily of enzymes including 11 families (PDE1–11) with several different genes and splice variants generating close to 100 isozymes showing unique kinetic, regulatory, and subcellular localization properties.[14] PDEs play a pivotal role in shaping local cAMP signals by limiting cAMP diffusion beyond a microdomain and by regulating cAMP levels within a microdomain. As a consequence, inhibition of individual PDE families results in a compartmentalized increase in cAMP as shown by studies using targeted reporters and real-time imaging of cAMP levels in intact myocytes.[15,16]

We have previously reported that in intact neonatal rat ventricular myocytes (NRVMs), PDE2, PDE3, and PDE4 are localized at distinct subcellular sites and uniquely modulate the cAMP response to individual extracellular stimuli.[17,18] In NRVM cell lysates, PDE3 and PDE4 account for most of the PDE activity, whereas PDE2 is responsible for only a minor fraction of cAMP hydrolytic activity.[17] However, in intact NRVMs, in spite of its low abundance, PDE2 plays a major role in the control of the cAMP response to catecholamines,[18] an effect that relies on its specific localization within the cell.[16]

Although the concept of compartmentalized cAMP/PKA signaling in cardiac myocytes is well established and the physiological function downstream of individual cAMP pools is being elucidated,[10,11,19,20] little is known about the role of local cAMP pools in the pathogenesis of heart disease. Catecholamines induce cardiac hypertrophy via mechanisms that include activation of β-adrenergic receptors, generation of cAMP, and PKA-mediated elevation of intracellular Ca^{2+}.[21] Although chronic stimulation of β-adrenergic signaling leads to pathological sequelae, enhancement of particular aspects of cAMP/PKA signaling benefits the failing heart,[22–24] suggesting that different components of this pathway may have different consequences on cardiac hypertrophy and failure.

In this study, we investigate the effect on cardiac hypertrophy of local manipulation of cAMP levels via selective inhibition of individual PDEs. We find that distinct pools of cAMP affect cardiac myocyte hypertrophic growth differently and that inhibition of PDE2, unlike inhibition of PDE3 or PDE4, results in antihypertrophic effects both in vitro and in vivo. We further demonstrate that increased PDE2 activity is sufficient per se to induce hypertrophy. The antihypertrophic effect of PDE2 inhibition relies on a local increase in cAMP that enhances PKA-mediated phosphorylation of nuclear factor of activated T cells (NFAT) and its consequent retention in the cytosol. We conclude that PDE2 regulates a pool of cAMP with unique effects on cardiac myocyte hypertrophic growth and identify PDE2 as a potential therapeutic target.

Methods

A detailed description of the Materials and Methods is included in the Online Data Supplement to this article.

Results

PDE2 Inhibition Counteracts Cardiac Myocyte Hypertrophy In Vitro and In Vivo

Treatment of NRVMs with 10 μmol/L norepinephrine for 48 hours is a well-established in vitro model of cardiac hypertrophy[25] eliciting the expected hypertrophy markers, including increase in cell surface area,^{3}H-leucine incorporation, nuclear translocation of NFAT (Figure 1B–1D), and atrial natriuretic peptide levels (Online Figure IA). To investigate the effect of raising cAMP levels on cardiac myocyte hypertrophy, we treated NRVMs with different cAMP-raising agents (Figure 1A). Activation of adenylyl cyclase with 1 μmol/L forskolin, inhibition of PDE4 with 10 μmol/L rolipram, and inhibition of PDE3 with 10 μmol/L cilostamide generated significant hypertrophy (Figure 1B–1D). In contrast, inhibition of PDE2 with BAY 60-7550 (10 μmol/L) did not induce hypertrophy (Figure 1B–1D), despite generating an increase in cAMP (Figure 1A). The unique effect of PDE2 inhibition on cell hypertrophy was also apparent in cells co-treated with norepinephrine. When cilostamide and rolipram were administered in combination with 10 μmol/L norepinephrine, norepinephrine further increased cell size compared with inhibitor alone, although no further enhancement of hypertrophy was observed compared with norepinephrine alone (compare Figure 1B–1D and 1F–1I). In contrast, BAY 60-7550 blocked the hypertrophic growth induced by norepinephrine (Figure 1F–1I and Online Figure IA–IF), despite its potentiation of the norepinephrine-induced

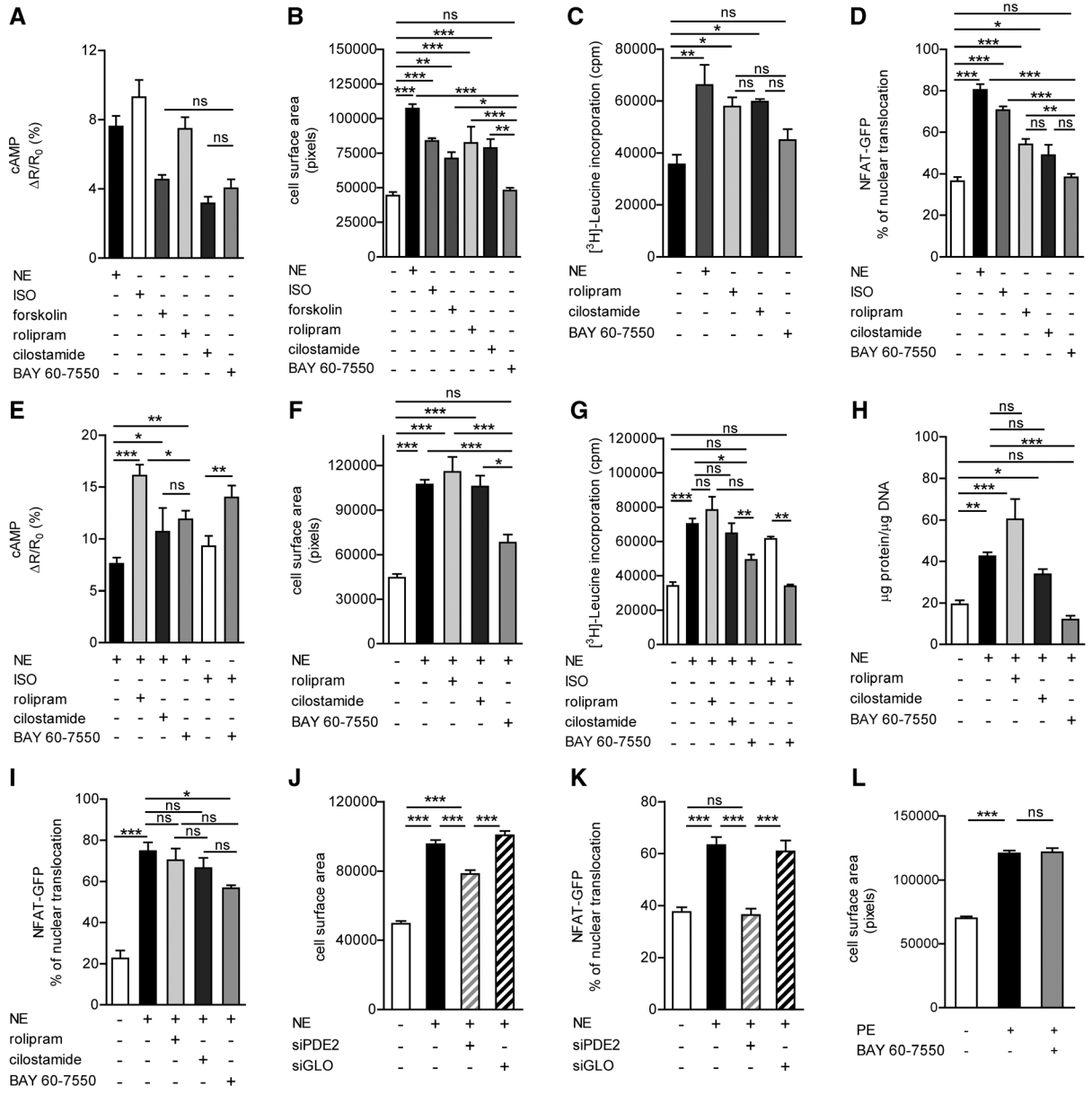

Figure 1. Effect of phosphodiesterase 2 (PDE2) inhibition on cardiac myocyte hypertrophy in vitro. A, cAMP increase induced by 1 nmol/L norepinephrine (NE), 10 nmol/L isoproterenol (ISO), 1 µmol/L forskolin, 10 µmol/L rolipram, 10 µmol/L cilostamide, or 10 µmol/L BAY 60-7550 measured in neonatal rat ventricular myocytes (NRVMs) using real-time fluorescence resonance energy transfer (FRET) imaging (n≥4 cells). **B**, Cell surface area of NRVMs treated for 48 hours with NE (10 µmol/L), ISO (10 µmol/L), forskolin (1 µmol/L), rolipram (10 µmol/L), cilostamide (10 µmol/L), and BAY 60-7550 (10 µmol/L) or untreated control. n≥32 cells. [3H] leucine incorporation (n≥16 independent experiments; **C**) and nuclear factor of activated T cells (NFAT)-green fluorescent protein (GFP) nuclear translocation measurements (minimum of 3 independent experiments; **D**) calculated for untreated NRVMs or NRVMs treated as indicated. **E**, FRET measurements of cAMP levels in NRVMs on stimulation with NE (1 nmol/L) and NE in combination with 10 µmol/L rolipram, 10 µmol/L cilostamide, or 10 µmol/L BAY 60-7550. Cell surface area (n≥44 cells; **F**), [3H] leucine incorporation (n≥27 independent experiments; **G**), normalized protein content (**H**) and NFAT-GFP nuclear translocation (**I**) measured in NRVMs untreated or treated for 48 hours as indicated. Cell surface area (minimum of n=128 cells per condition; **J**) and NFAT-GFP nuclear translocation (minimum of 5 independent experiments; **K**) for control, NE (10 µmol/L)-treated NRVMs, and NRVMs treated with NE (10 µmol/L) and transfected either with siPDE2 (small interference RNA for PDE2) or with the control oligo siGLO Red. **L**, Cell surface area of NRVMs treated for 48 hours as indicated; phenylephrine (PE; 1 µmol/L), BAY 60-7550 (10 µmol/L); n≥135 cells. All data represent mean±SEM. One-way ANOVA and Tukey's multiple comparison tests were performed. Pixel size =0.1075 µm. *P≤0.05; **P≤0.01; ***P≤0.005; ns=not significant.

cAMP response (Figure 1E). The antihypertrophic effect of BAY 60-7550 was confirmed at 50 nmol/L of inhibitor (Online Figure IB). Similar results were found with erythro-9-(2-hydroxy-3-nonyl)adenine, another selective PDE2 inhibitor (Online Figure IC), in cardiomyocytes from neonatal mice (Online Figure ID) and in adult rat ventricular myocytes (ARVMs) (Online Figure IE and IF). Similar effects on cell size (Figure 1J) and NFAT-green fluorescent protein (GFP) nuclear translocation (Figure 1K) were found when PDE2 expression was knocked down using the small interfering RNA

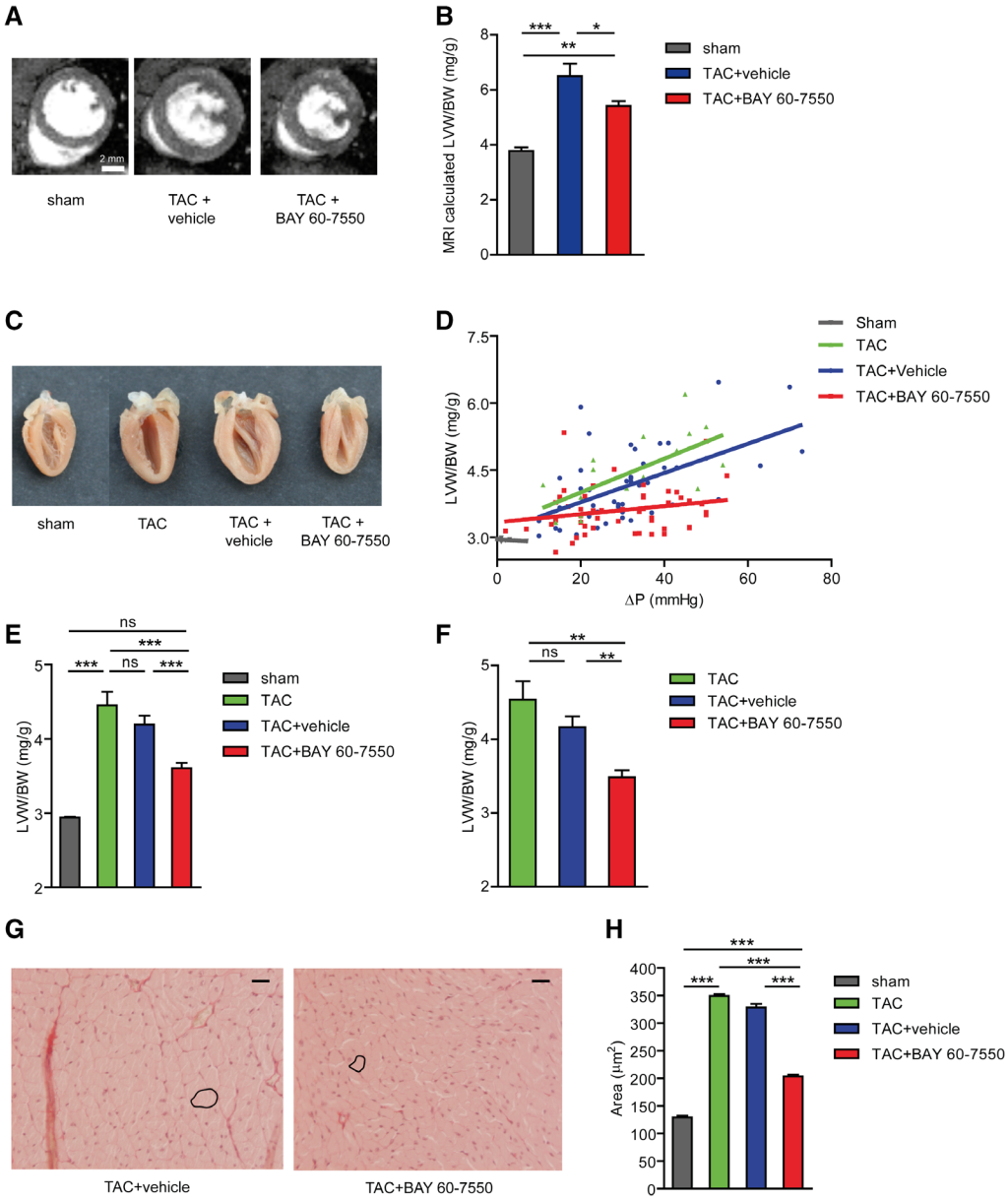

Figure 2 . Phosphodiesterase 2 (PDE2) inhibition attenuates cardiac hypertrophy in vivo. A, Representative mid-ventricular magnetic resonance imaging (MRI) short-axis images of left ventricle in end diastole treated for 3 weeks as indicated. **B**, Left ventricular weight (LVW) calculated from MRI recordings divided by body weight (BW) as indicated. n=4 to 8 mice per group. **C**, Representative heart sections obtained from mouse hearts extracted 3 weeks after sham or transverse aorta constriction (TAC) operation in the absence or presence of treatment, as indicated. **D**, LVW/BW ratio plotted against the systolic pressure gradient calculated as a difference between right and left carotid systolic blood pressure (ΔP) at 3 weeks after sham operation, TAC, TAC+vehicle, or TAC+BAY 60-7550 (3 mg/kg). **E**, Summary and comparison of mean LVW/BW ratio values calculated for all sham-operated, TAC-, TAC+vehicle–, or TAC+BAY 60-7550–treated mice. **F**, Mean LVW/BW ratio values calculated for TAC-, TAC+vehicle–, or TAC+BAY 60-7550–treated mice presenting with a ΔP within the 30 to 40 mm Hg range. **G**, Representative images of picrosirius red staining of heart sections generated after 3 weeks of TAC and treatment with vehicle or BAY 60-7550. In each panel, the contour of a representative cell is highlighted with a black line. Scale bar =40 μm. **H**, Summary of myocyte cross-sectional area from sham-, TAC-, TAC+vehicle–, and TAC+BAY 60-7550–treated hearts (mean±SEM of at least n=213 cells per condition). One-way ANOVA and Tukey's multiple comparison tests were performed in all the experiments. *$P \leq 0.05$; **$P \leq 0.01$; ***$P \leq 0.005$.

sequence siPDE2 (small interference RNA for PDE2).[16] The specificity of the small interfering RNA effect was confirmed by rescue experiments (Online Figure II). BAY 60-7550 also blocked the hypertrophy induced by treatment with 10 μmol/L isoproterenol (Figure 1G), whereas it had no effect on the hypertrophy induced by phenylephrine (Figure 1L), indicating that PDE2 acts downstream of the β- rather than the α-adrenergic receptor. Consistently, Bay 60-7550 did not inhibit phenylephrine-induced NFAT nuclear translocation (Online Figure IG) and did not affect the nuclear translocation of NFAT in response to phenylephrine and selective inhibition of GSK3β (glycogen synthase kinase 3 beta) and JNK (c-Jun N-terminal kinases) (Online Figure IG), indicating that inhibition of PDE2 acts independently of this pathway.

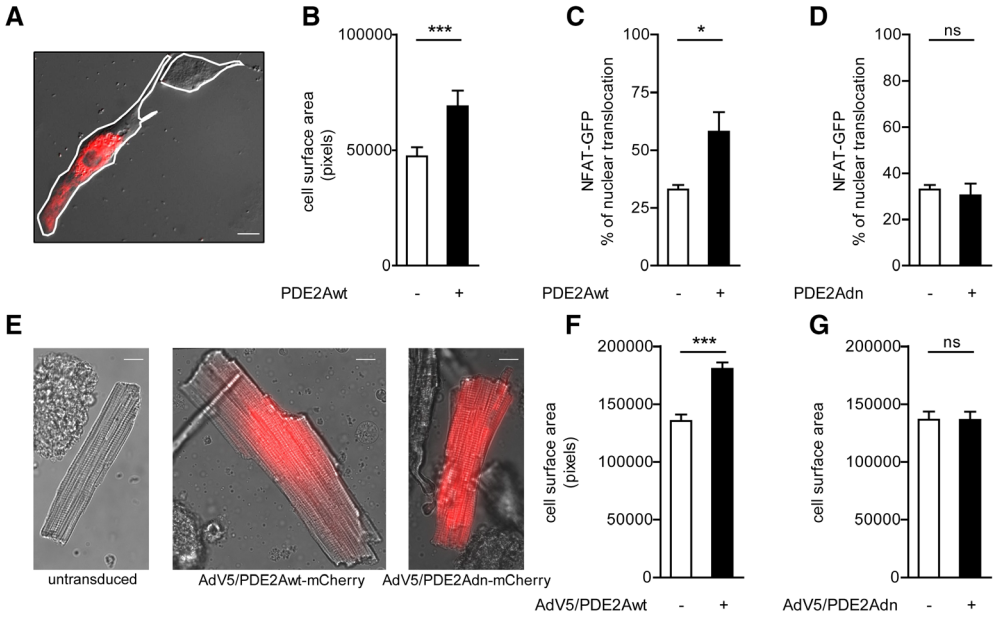

Figure 3. Phosphodiesterase 2 (PDE2) overexpression induces cardiac myocyte hypertrophic growth in vitro and in vivo. A, Overlay of differential interference contrast (DIC) and fluorescence images showing in the same field one neonatal rat ventricular myocytes (NRVM) overexpressing Red fluorescent protein–tagged version of PDE2 (PDE2Awt-mRFP) and one untransfected control cardiomyocyte. Cell contour is highlighted in white (Scale bar: 10 μm). **B**, Cell surface area (3 independent experiments, n≥49) calculated for untransfected NRVMs or NRVMs overexpressing PDE2Awt-mRFP (pixel size =0.1075 μm). **C and D**, Percentage of cells showing nuclear translocation of nuclear factor of activated T cells (NFAT)-GFP measured for untransfected control NRVMs and NRVMs overexpressing PDE2Awt-mRFP or PDE2A2dn-mRFP (dominant negative phosphodiesterase 2-monomeric red fluorescent protein; 4 independent experiments, total cell number ≥47). **E**, Representative images of untransduced (**left**) and transduced ARVMs expressing adenoviral vector (Ad) expressing the PDE2A enzyme tagged with mCherry (AdV5/PDE2Awt-mCherry; **middle**) or the catalytically inactive ADV5/PDE2Adn-mCherry (adeno virus 5-dominant negative phosphodiesterase 2-monomeric cherry; **right**). **F**, Summary of cell surface area of ARVMs transduced with AdV5/PDE2wt-mCherry and untransduced myocytes isolated from the same heart. **G**, Cell surface area of ARVMs obtained from hearts injected with AdV5/PDE2Adn-mCherry and expressing or not expressing the catalytically inactive recombinant enzyme. Consistent results were obtained from hearts from 3 different animals injected with AdV5/PDE2Awt-mcherry and 3 animals injected with AdV5/PDE2Adn-mcherry; number of cells for each condition was ≥100. Pixel size =0.1613 μm. All data represent mean±SEM. For all experiments, *t* test statistical analysis was performed. **P*≤0.05, ****P*≤0.005.

To examine whether PDE2 inhibition also attenuates cardiac hypertrophy in vivo, adult C57Bl/6 mice were subjected to transverse aorta constriction (TAC) for 3 weeks and concurrently treated with BAY 60-7550 (3 mg/kg) or with vehicle (Online Table I). The PDE2 inhibitor induced a significant reduction of cardiac hypertrophy as verified by echocardiography (Online Figure I-H and I-I), cardiac magnetic resonance imaging (Figure 2A and 2B), and postmortem examination (Figure 2C–2H).

PDE2 overexpression results in cardiac myocyte hypertrophy both in vitro and in vivo. We next investigated the effect of increasing PDE2 activity in NRVMs by overexpressing a red fluorescent protein–tagged version of PDE2 (PDE2Awt-mRFP). We found a significant increase in cell surface area (Figure 3A and 3B) and in nuclear translocation of NFAT-GFP (Figure 3C) in transfected versus untransfected cells. Overexpression of a catalytically inactive version of the enzyme (dnPDE2Awt-mRFP) had no effect (Figure 3D and 5E). Similar results were found in ARVMs (Online Figure IIIA). To test whether overexpression of PDE2 results in hypertrophic growth in vivo, a recombinant adenoviral vector (Ad) expressing the PDE2A enzyme tagged with mCherry (AdV5/PDE2Awt-mCherry) was injected in the heart of adult rats. Seven days after injection, the cell surface areas of transduced and untransduced myocytes dissociated from the same heart were compared. As shown in Figure 3E and 3F, PDE2Awt-mCherry-expressing cardiomyocytes show a significant increase in cell surface area as compared with untransduced cells; cardiomyocytes overexpressing the catalytically inactive PDE2Adn-mCherry did not differ from untransduced cells (Figure 3E and 3G).

Antihypertrophic Effect of PDE2 Inhibition Is PKA-Dependent

PDE2 can degrade both cAMP and cyclic GMP[26]; therefore, its inhibition may result in an increase of both second messengers. To establish whether PKA or protein kinase G mediates the antihypertrophic effect of PDE2 inhibition, we measured cell surface area and NFAT-GFP nuclear translocation in norepinephrine-treated NRVMs in the presence of selective kinase inhibitors. The selective protein kinase G inhibitor DT-2[27] did not affect the ability of BAY 60-7550 to significantly reduce hypertrophy (Figure 4A and 4B). As a control, we measured the effect of DT-2 on the antihypertrophic effect of selective inhibition of the cyclic GMP–specific PDE5 with sildenafil (10 nmol/L), previously reported to counteract hypertrophy via protein kinase G activity.[28] We found that sildenafil alone had no effect on either cell surface area or NFAT-GFP nuclear translocation (Online Figure IV), but DT-2 completely blocked the cyclic GMP–mediated

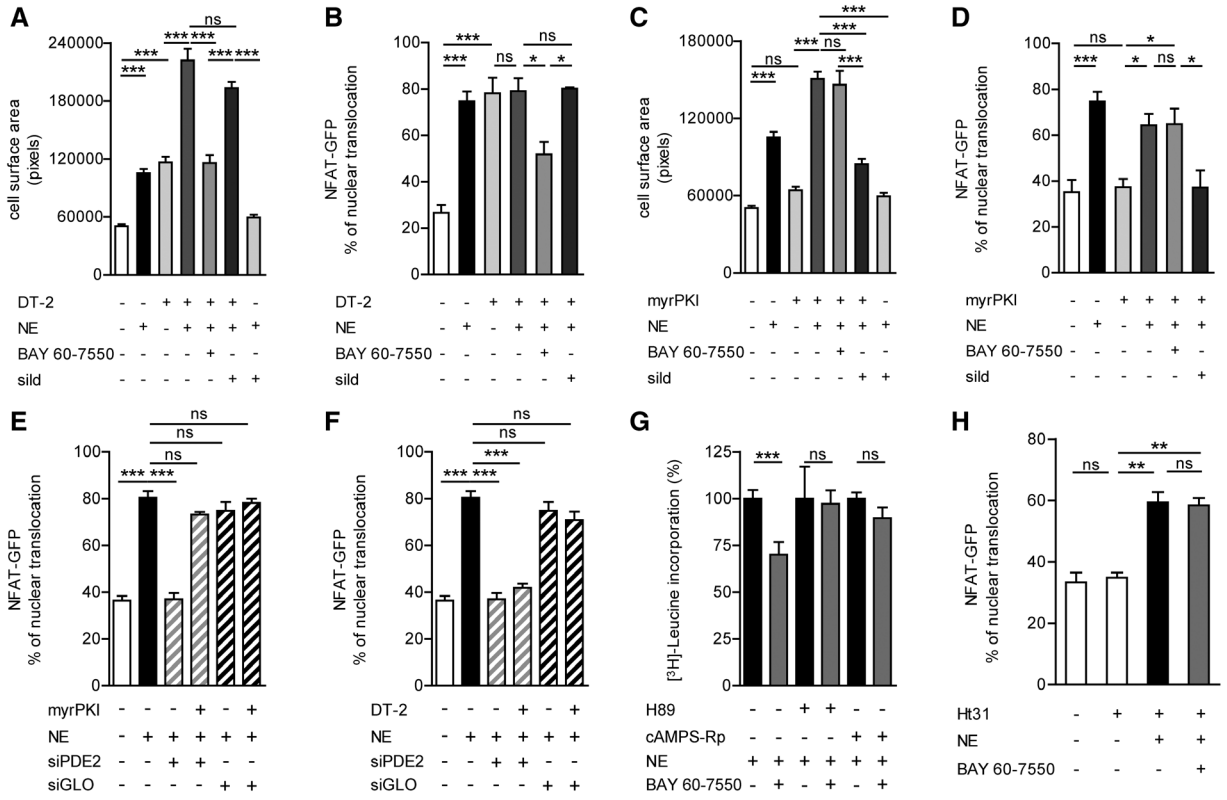

Figure 4. The antihypertrophic effect of phosphodiesterases 2 (PDE2) inhibition is protein kinase A (PKA)–dependent. Cell surface area (3 independent experiments, n≥72; **A**) and nuclear factor of activated T cells (NFAT)-GFP nuclear translocation (3 independent experiments, n ≥50; **B**) measurements for untreated control, neonatal rat ventricular myocytes (NRVMs) treated for 48 hours with norepinephrine (NE; 10 μmol/L) or DT-2 (10 μmol/L) or treated with DT-2 in combination with NE, NE and BAY 60-7550 (10 μmol/L), or NE and sildenafil (10 nmol/L) as indicated. Cell surface area (3 independent experiments, n≥54; **C**) and percentage of NFAT-GFP nuclear translocation (4 independent experiments, n ≥76; **D**) calculated for untreated control, NRVMs treated for 48 hours with NE (10 μmol/L) or myristoylated protein kinase A inhibitor peptide (myrPKI) alone (10 μmol/L), or treated in combination with NE, NE and BAY 60-7550 (10 μmol/L), or NE and sildenafil (10 nmol/L) as indicated. **E and F**, NFAT-GFP nuclear translocation measurements (3 independent experiments) for untreated control, NE (10 μmol/L)-treated NRVMs, or NRVMs treated with NE (10 μmol/L) and transfected either with siPDE2 or with the control oligo siGLO Red in the presence or absence of DT-2 (10 μmol/L) or of myrPKI (10 μmol/L). **G**, [3H] leucine incorporation assay performed in NRVMs treated with NE in combination with BAY 60-7550 (10 μmol/L) and the PKA inhibitors H89 or cAMPS-Rp (n≥4 independent experiments). **H**, NFAT-GFP nuclear translocation measurements (2 independent experiments) for untreated control and NRVMs transfected with Ht31 and treated with NE and BAY 60-7550. All data represent mean±SEM. One-way ANOVA and Tukey's multiple comparison tests were used. Pixel size =0.1075 μm. **P*≤0.05, ***P*≤0.01, ****P*≤0.005.

effect of sildenafil on norepinephrine-induced cell size increase (Figure 4A) and NFAT-GFP nuclear translocation (Figure 4B). In contrast, selective PKA inhibition with myristoylated protein kinase A inhibitor peptide (myrPKI)[29] completely abolished the antihypertrophic effects of BAY 60-7550 (Figure 4C and 4D) without affecting the antihypertrophic effect of sildenafil (Figure 4C and 4D). In keeping with these findings, the effect of PDE2 knockdown on norepinephrine-induced hypertrophy was completely blocked by myrPKI but was unaffected by DT-2 treatment (Figure 4E and 4F). Consistent with a role for PKA activation downstream of PDE2 inhibition, we found that Bay 60-7550 significantly increases PKA-mediated phosphorylation of the fluorescence resonance energy transfer reporter AKAR4 (A kinase activity reporter 4) (Online Figure V). The role of PKA is further supported by the finding that the antihypertrophic effect of BAY 60-7550 is completely blocked by the PKA inhibitors H89 and cAMPS-Rp (Figure 4G). In addition, we found that disrupting PKA–AKAPs interactions with the competing peptide Ht31[30] abolishes the effect of BAY 60-7550 on nuclear translocation of NFAT (Figure 4H), confirming a PKA-dependent mechanism and indicating that a localized subset of PKA is involved. Thus, the antihypertrophic effect of PDE2 is PKA-mediated and protein kinase G–independent.

PDE2 Modulates a Local Pool of cAMP With Antihypertrophic Effects

PDE2 has been shown to be targeted to specific subcellular sites in NRVMs,[18] a finding that we confirm here in ARVMs (Online Figure VI). A possible explanation for the opposite effect on cell size observed on selective PDE inhibition is that blocking the activity of a localized PDE2 raises cAMP content in a specific subcellular microdomain that is linked to antihypertrophic effects, whereas inhibition of PDE3 and PDE4 increases cAMP at sites where prohypertrophic effectors are activated. If so, it should be possible to recapitulate the effect of selective pharmacological inhibition by displacing the individual PDEs from their anchor

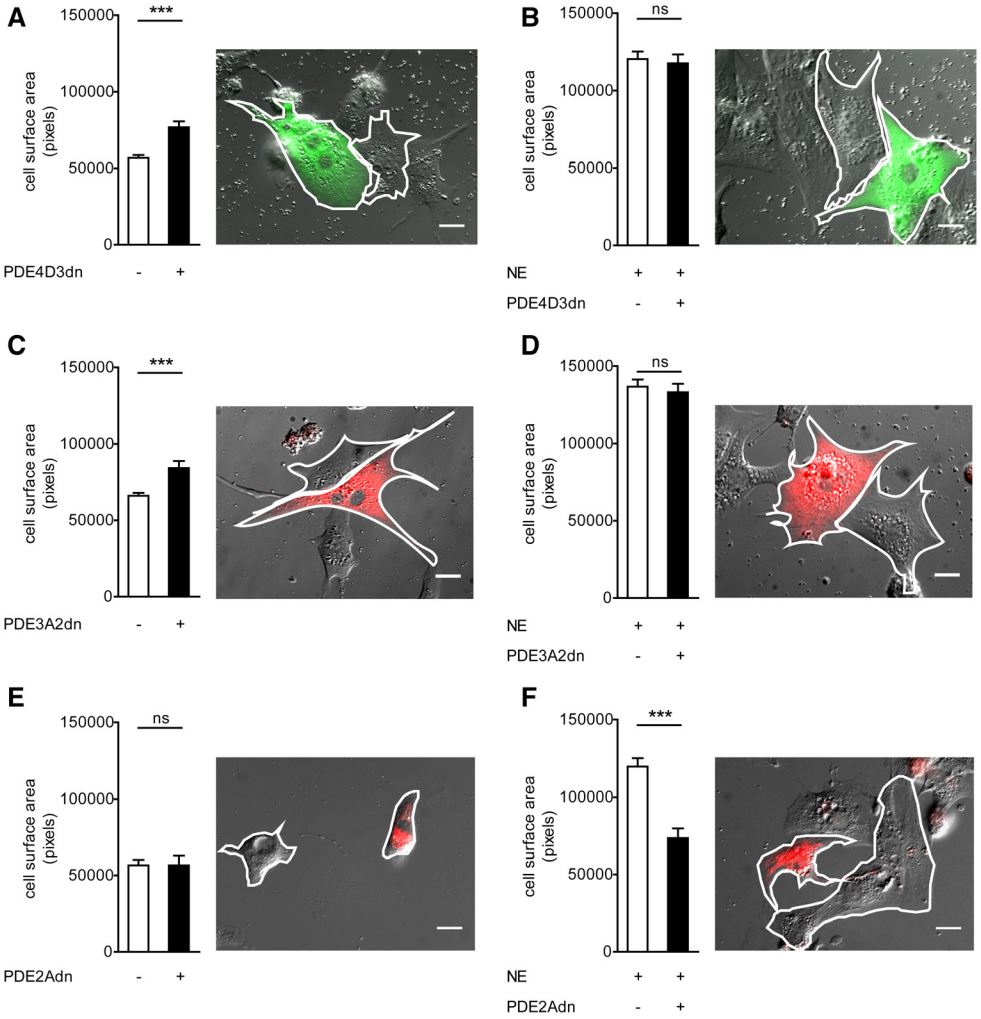

Figure 5 . Phosphodiesterases 2 (PDE2) modulates a local pool of cAMP with antihypertrophic effects. Neonatal rat ventricular myocytes (NRVM) were transfected with catalytically inactive PDE4D3 (**A and B**), catalytically inactive PDE3A2 (**C and D**), or catalytically inactive PDE2A (**E and F**), and cell surface area was measured in the absence or presence of 10 μmol/L norepinephrine (NE) for 48 hours. In each panel, the cell surface area is shown as mean±SEM on the left, and on the right, an overlay of differential interference contrast (DIC) and fluorescence images showing one NRVM overexpressing the catalytically inactive PDE and in the same field a nontransfected control cardiomyocyte is presented. For all conditions, n≥25 cells from 3 independent experiments. Pixel size =0.1075 μm. Scale bar: 10 μm. For all experiments, *t* test statistical analysis was performed. ***$P \leq 0.005$; ns=not significant.

sites within the cell, a maneuver that has been previously used to generate a localized increase in cAMP.[16,31] To test this, we measured cell surface area in NRVMs overexpressing fluorescent protein–tagged chimeras of catalytically inactive mutants of PDE2A (PDE2Adn),[16] PDE3A2 (PDE3A2dn), and PDE4D3 (PDE4D3dn).[32] We found that displacement of endogenous PDE4D3 (Figure 5A) or PDE3A2 (Figure 5C) resulted in hypertrophy and did not further increase the hypertrophy induced by norepinephrine treatment (Figure 5B and 5D), reproducing the effects of pharmacological inhibition. In contrast, displacement of endogenous PDE2A did not affect cell size in untreated myocytes (Figure 5E), but significantly reduced the hypertrophy induced by norepinephrine (Figure 5F). Similar results were found for nuclear translocation of NFAT-GFP (Online Figure VIIA and VIIB) and in ARVMs (Online Figure VIIC–VIIF). These data support a model whereby different PDEs localized to different intracellular locations control distinct pools of cAMP with opposite effects on cardiac myocyte cell size.

Antihypertrophic Effect of PDE2 Inhibition Is Mediated by PKAII

The data presented to date demonstrate that a local pool of cAMP with antihypertrophic effects is selectively regulated by PDE2-mediated hydrolysis. To gain some insight into the subcellular localization of such a pool, we measured the cAMP signal generated on selective PDE2 inhibition using RI_epac and RII_epac, 2 fluorescence resonance energy transfer–based reporters for cAMP that localize to the sites where PKAI and PKAII, respectively, normally reside within the cell. These reporters target to different AKAPs and selectively detect cAMP signals within distinct subcellular compartments.[6] PDE2 inhibition potentiates the cAMP response to 10 nmol/L norepinephrine (Figure 6A)

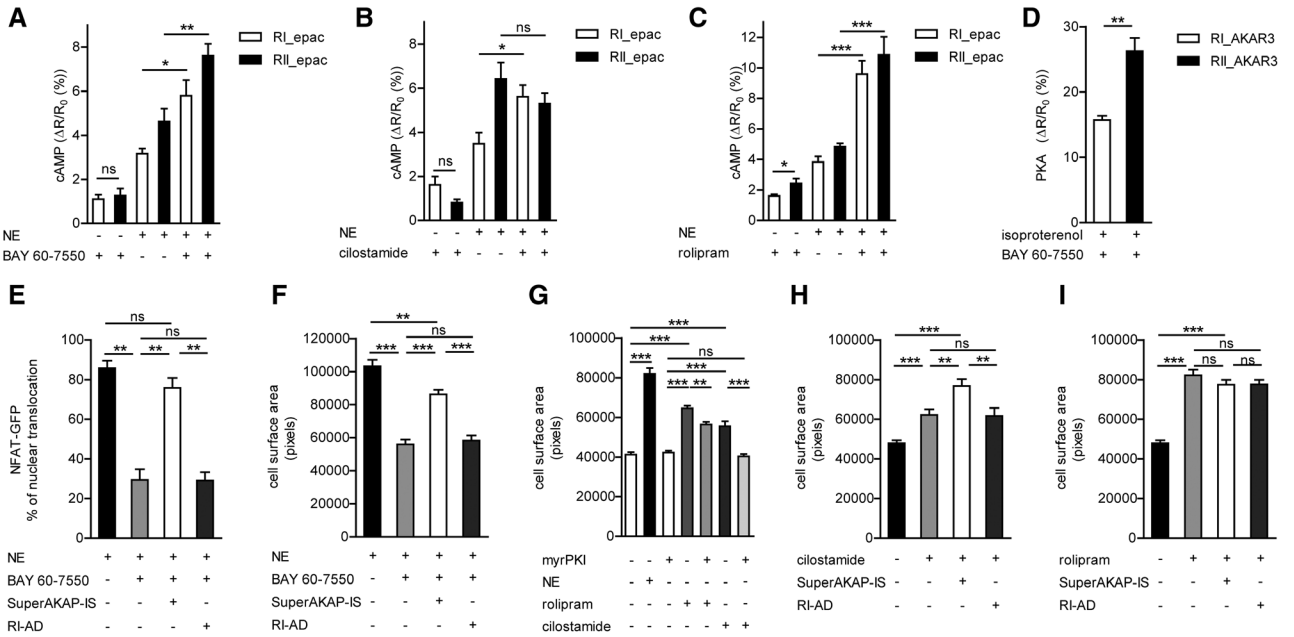

Figure 6 . Protein kinase A type II (PKAII) mediates the antihypertrophic effects of BAY 60-7550. Quantification of cAMP changes induced by BAY 60-7550 (10 μmol/L), norepinephrine (NE; 10 nmol/L), NE plus BAY 60-7550 **(A),** or by cilostamide (10 μmol/L), NE (10 nmol/L), or NE plus cilostamide **(B)**, or by rolipram (10 μmol/L), NE (10 nmol/L), or NE plus rolipram **(C)** in neonatal rat ventricular myocytes (NRVMs) expressing either RI-epac or RII-epac. n≥4. **D**, Quantification of PKA isoform-selective activation induced by isoproterenol (10 nmol/L) and BAY 60-7550 measured in NRVMs expressing the FRET sensors RI_AKAR3 or RII_AKAR3 (regulatory I_A kinase activity reporter 3 or regulatory II_A kinase activity reporter 3).[16] n≥3. **E**, Percentage of cells showing nuclear translocation of nuclear factor of activated T cells (NFAT)-GFP **(F)** and cell size measured for NE-treated or NE+BAY 60-7550–treated NRVMs untransfected or transfected with either SuperAKAP-IS or RI-AD. n≥4. **G**, Cell surface area measurements of NRVMs treated for 48 hours as indicated. Cell size measured for untransfected NRVMs or NRVMs transfected with either super A kinase Anchoring protein-in silico (SuperAKAP-IS) or RI-AD and treated with cilostamide **(H)** or rolipram **(I)** as indicated; n≥34. All data represent mean±SEM. For experiments in **A**–**D**, a *t* test statistical analysis was performed. In **E**–**I**, 1-way ANOVA and Tukey's multiple comparison tests were used. ***P≤0.005; **P≤0.01; *P≤0.05; ns=not significant.

or 10 nmol/L isoproterenol (Online Figure VIIIA), both in the PKAI and PKAII compartments, whereas PDE3 inhibition affects the cAMP response exclusively in the PKAI compartment (Figure 6B and Online Figure VIII B). Similar results were found in ARVM (Online Figure VIIID and VIIIE). As inhibition of PDE3 promotes, rather than inhibits, hypertrophy (Figure 1A and 1D), we hypothesized that the cAMP pool under the control of PDE2 and responsible for the antihypertrophic effect is associated with the PKAII compartment. Consistent with this model, we found that, on inhibition of PDE2, PKA-mediated phosphorylation is significantly higher in the PKAII compartment as opposed to the PKAI compartment (Figure 6D). In addition, the effect of PDE2 inhibition on hypertrophy was completely blocked by super A kinase Anchoring protein-in silico (SuperAKAP-IS),[12] a peptide that disrupts selectively the interaction between PKAII and AKAPs, whereas the PKAI–AKAP selective disruptor regulatory I anchoring disruptor (RIAD)[33] had no effect (Figure 6E and 6F), confirming that a subset of AKAP-anchored PKAII mediates the antihypertrophic effect downstream of PDE2 inhibition. Interestingly, the prohypertrophic effects of PDE3 and PDE4 inhibition, although PKA-dependent (Figure 6G), were not affected by treatment with either SuperAKAP-IS or RIAD (Figure 6H and 6I), suggesting that the prohypertrophic effect of PDE3 and PDE4 inhibition does not require an AKAP-anchored subset of PKA.

Antihypertrophic Effect of PDE2 Inhibition Requires PKA-Mediated Phosphorylation of NFAT

Nuclear translocation of NFAT regulates pathological cardiac hypertrophy.[34] PKA phosphorylates NFAT at Ser 245, Ser 269, and Ser 294,[35] thus preventing its nuclear translocation.[36] We therefore hypothesized that the antihypertrophic effects of PDE2 inhibition may rely on PKA-mediated phosphorylation of NFAT. Consistent with our hypothesis, treatment of NRVM with Bay 60-7550 results in strong enhancement of PKA-dependent phosphorylation of NFAT both in nonhypertrophic (Figure 7A) and norepinephrine-hypertrophyed (Figure 7B) cells. In addition, in a pull-down of PKA-phosphorylated proteins from lysates of NRVMs hypertrophied in vitro, the amount of PKA-phosphorylated NFAT-GFP was significantly higher in BAY 60-7550–treated than in control cells (Online Figure IXC and IXD). Similar results were obtained from NFAT-GFP pull-downs probed with a PKA substrate antibody (Online Figure IXA and IXB). Notably, increased phosphorylation on inhibition of PDE2 was confirmed when probing for endogenous NFAT (Figure 7C). It is interesting to note that PDE4 inhibition increases PKA-mediated phosphorylation of overexpressed NFAT-GFP (Figure 7B and Online Figure IXC and IXD), in line with the large global rise in cAMP that it generates (Figure 1C). Overexpressed NFAT is likely to distribute to sites where endogenous NFAT normally is not present, and therefore, it is expected to become phosphorylated on PDE4 inhibition. However, PDE4 inhibition does not

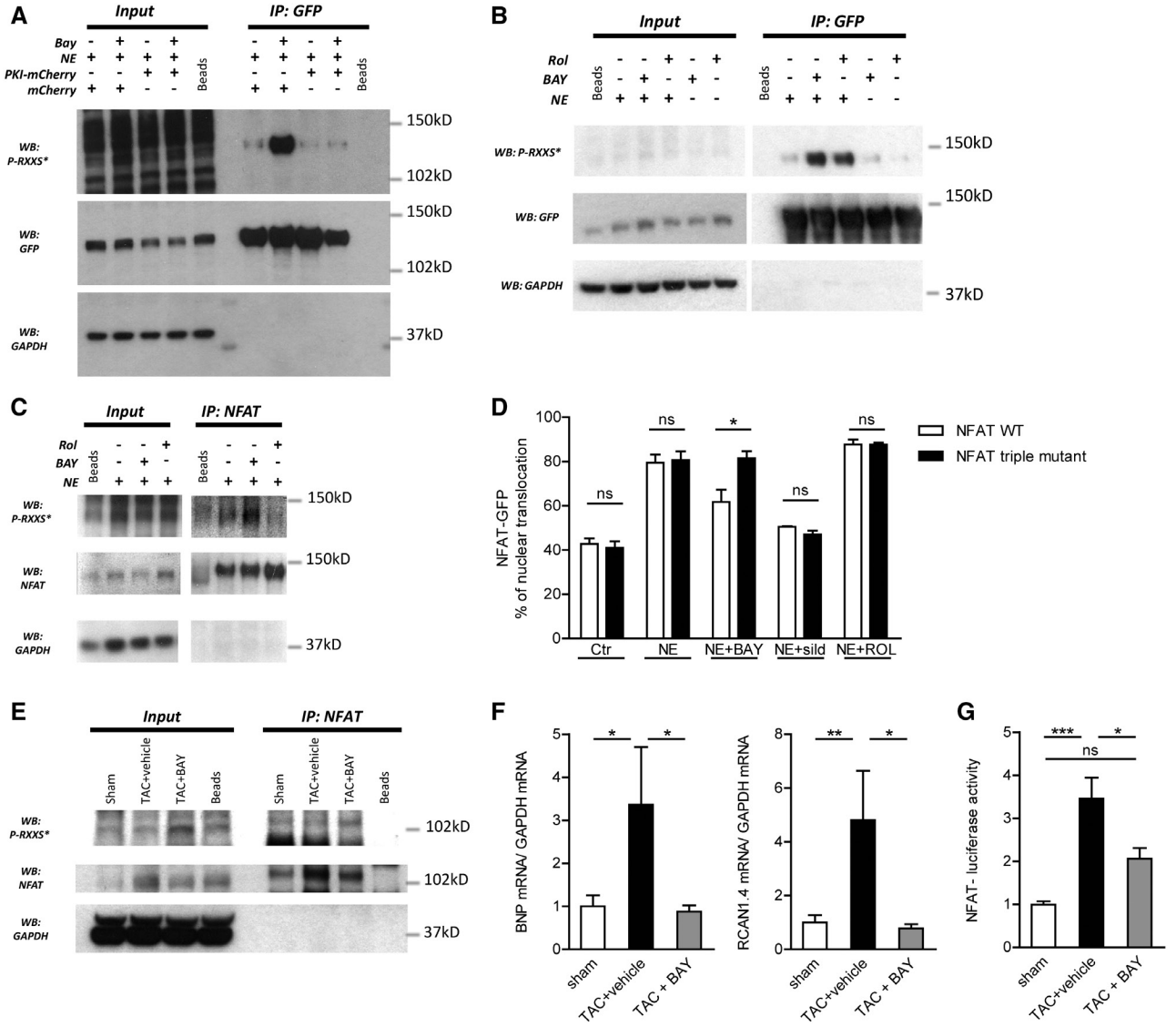

Figure 7 . The antihypertrophic effect of phosphodiesterases 2 (PDE2) inhibition requires protein kinase A (PKA)–mediated phosphorylation of nuclear factor of activated T cells (NFAT). A, Representative GFP-pull down experiment from lysate of neonatal rat ventricular myocytes (NRVMs) expressing NFAT-GFP, PKI-mCherry, or mCherry. Cells were treated for 10 minutes with norepinephrine (NE; 10 μmol/L) and BAY 60-7550 (10 μmol/L) as indicated. Blots were probed with anti-phospho-PKA substrate, anti-GFP, and anti-GAPDH antibodies. n=3. **B**, Representative GFP-pull down experiment from lysate of NRVMs expressing NFAT-GFP and treated for 48 hours with NE (10 μmol/L), BAY 60-7550 (10 μmol/L), and rolipram (10 μmol/L) as indicated. Blots were probed with anti-phospho-PKA substrate, anti-GFP, and anti-GAPDH antibodies. n=3.**C**, Representative immunoprecipitation of endogenous NFAT performed on lysates from NRVMs treated for 48 hours with NE, BAY 60-7550, and rolipram as indicated. Blots were probed with anti-phospho-PKA substrate, anti-NFAT, and anti-GAPDH antibodies. n=3. **D**, Nuclear translocation of NFAT-GFP wild-type or NFAT-GFP triple mutant (S245A/S269A/S294A) calculated for untreated NRVMs, NRVMs treated for 48 hours with NE (10 μmol/L), NE and BAY 60-7550 (10 μmol/L), NE and sildenafil (10 nmol/L), or NE and rolipram (10 μmol/L); n=3 independent experiments. **E**, Representative immunoprecipitation of endogenous NFAT performed on mouse left ventricles whole cell lysates from sham, transverse aorta constriction (TAC)+vehicle, or TAC+BAY 60-7550 mice as indicated. Blots were probed with anti-phospho-PKA substrate, anti-NFAT, and anti-GAPDH antibodies. Representative of 4 independent experiments, **F**, B natriuretic peptide (BNP; **left**) and regulator of calcineurin 1 (RCAN1.4; **right**) mRNA levels measured in left ventricular (LV) samples from sham, TAC+vehicle, or TAC+BAY 60-7550 mice as indicated (n=3–7). **G**, Quantification of NFAT luciferase activity in LV homogenates from NFAT luciferase reporter mice subjected to TAC and 2 weeks treatment with BAY 60-7550 or vehicle, normalized to sham values. Four repeats per sample were performed. All data represent mean±SEM. In **D**, *t* test was utilized. One-way ANOVA and Tukey's multiple comparison tests were performed in **F** and **G**. Pixel size =0.1075 μm. **P*≤0.05; ***P*≤0.01; ns=not significant.

significantly affect the phosphorylation of endogenous NFAT (Figure 7C), further confirming that PDE2 and PDE4 act on distinct pools of cAMP and have distinct effects on the endogenous protein.

To further test whether the antihypertrophic effect of BAY 65-7550 is mediated by PKA-dependent phosphorylation of NFAT, we generated a PKA phosphorylation-resistant form of NFAT-GFP by introducing serine-to-alanine substitutions at positions 245, 269, and 294. BAY 60-7550 reduced the translocation of wild-type NFAT-GFP, but did not affect nuclear translocation of triple-mutant NFAT-GFP (Figure 7D), indicating that the PKA phosphorylation sites on NFAT are

required for BAY 60-7550 to prevent norepinephrine-induced nuclear translocation of NFAT. In contrast, treatment of hypertrophic myocytes with sildenafil significantly blocked nuclear translocation of both wild-type and triple-mutant NFAT-GFP (Figure 7D), as expected given that the antihypertrophic effect mediated by sildenafil is independent of PKA phosphorylation (Figure 2 and Nickl et al[27]). Inhibition of PDE4 with rolipram did not affect the nuclear translocation of either wild-type or triple-mutant NFAT (Figure 7D). In further support of the role of a local pool of cAMP in the antihypertrophic effect of PDE2 inhibition, overexpression of PDE2Adn-mRFP in norepinephrine-treated NRVMs reduced nuclear translocation of NFAT-GFP (Online Figure XA) but not of triple-mutant NFAT-GFP (Online Figure XB). In addition, in the presence of triple-mutant NFAT-GFP, PDE2Adn-mRFP was unable to counteract norepinephrine-induced hypertrophy (Online Figure XC and XD), further confirming that the antihypertrophic effect of PDE2 requires PKA-mediated phosphorylation of NFAT. The involvement of NFAT phosphorylation and NFAT-dependent gene transcription in the antihypertrophic effect of PDE2 inhibition in vivo was confirmed in experiments where we measured NFAT phosphorylation (Figure 7E) and mRNA levels for BNP (B natriuretic peptide) and RCAN1 (regulator of calcineurin 1) (Figure 7F), 2 genes that are transcribed under the control of NFAT[34,37] in sham-operated, TAC+vehicle–treated, and TAC+BAY 60-7550–treated mice. We found that treatment with the PDE2 inhibitor significantly enhances NFAT phosphorylation and reduces the level of expression of NFAT-dependent genes, thus reversing the molecular fingerprint of pathological hypertrophy. To further support our conclusion that PDE2 inhibition counteracts cardiac hypertrophy in vivo via an NFAT-dependent mechanism, we subjected NFAT reporter mice[38] to TAC and randomization to treatment with BAY 60-7550 or vehicle for 2 weeks (Online Table II and Online Figure XI). In line with our previous results, BAY 60-7550–treated NFAT reporter mice showed reduced cardiac hypertrophy (Online Figure XI) and corresponding NFAT luciferase activity (Figure 7G) after TAC as compared with vehicle-treated mice.

Discussion

In this study, we identify PDE2 as a regulator of cardiac hypertrophy by providing strong evidence, in vitro and in vivo, that overexpression of PDE2 is sufficient per se to induce hypertrophy and that inhibition of PDE2 counteracts cardiac myocyte hypertrophic growth, an effect that relies on cAMP-dependent activation of PKA. Our data reveal a completely novel mechanism through which cAMP signaling impacts cardiac myocyte cell size that strictly depends on the subcellular site at which the cAMP signal is generated. Thus, inhibition of PDE2 generates a local pool of cAMP with antihypertrophic effects, whereas the rise in cAMP generated via inhibition of PDE3 or PDE4 has prohypertrophic effects. We demonstrate here for the first time that spatially distinct pools of cAMP can be generated downstream of βAR (beta adrenergic receptor) activation with opposing effects on myocyte size.

Using targeted fluorescence resonance energy transfer reporters for cAMP and selective displacement of PKAI and PKAII from their anchoring sites on AKAPs, we unveil a complex involvement of cAMP and PKA in the regulation of cardiac myocyte hypertrophy. Inhibition of PDE2 and of PDE4 increases cAMP in both the PKAI and PKAII compartments, yet the effect on cell size is opposite. To rationalize these findings, it should be noted that there are multiple PKAI–AKAP and PKAII–AKAP complexes in cardiac myocytes[7] and that the PKAI- and PKAII-targeted fluorescence resonance energy transfer reporters do not discriminate between individual complexes. Our findings support a model whereby a pool of cAMP generated in the PKAII compartment on PDE2 inhibition counteracts hypertrophy, whereas a pool of cAMP generated on inhibition of PDE4 within the PKAII compartment, but presumably involving different PKAII–AKAP complexes, has no effect on cell size. Alternatively, inhibition of PDE4 may affect the same pool of cAMP under the control of PDE2, but a concomitant increase in cAMP at a different site has a dominant, prohypertrophic effect. In support of the latter, using PKA–AKAP-selective disruptors, we find that inhibition of PDE4, as well as inhibition of PDE3, results in hypertrophy via activation of a subset of PKA that is not anchored to AKAPs.

It is well established that adrenergic stimulation can initiate cardiac hypertrophy via generation of cAMP and activation of PKA,[39,40] as confirmed by PKA knockout studies in which deletion of PKA subunits is protective against hypertrophy.[41] Other studies, however, have suggested that components of the β-adrenergic signaling pathway may play a protective role in response to hemodynamic overload. For example, it has been reported that overexpression of some types of adenylyl cyclase improve cardiac function[23] and that PKA-mediated phosphorylation of histone deacetylase 5 prevents its nuclear export and results in decreased cardiac myocyte size.[42] The present data support the coexistence within the same cell of multiple spatially segregated cAMP/PKA signaling pathways that can alternatively prevail depending on the status of the cell and provide a possible mechanistic basis for the dichotomy reported in the literature on the role of PKA on the development of cardiac pathology.

Dephosphorylation of NFAT and its subsequent translocation to the nucleus is regulated by the Ca^{2+}-calmodulin–dependent phosphatase, one of the most potent activators of the hypertrophic program.[34] Ca^{2+}-calmodulin–dependent phosphatase can directly interact with several AKAPs, including AKAP1,[43] AKAP5,[44] and AKAP6,[45] all of which bind PKA type II. In addition, studies suggest that regulation of Ca^{2+}-calmodulin–dependent phosphatase activity occurs via a specific microdomain of Ca^{2+},[46] further supporting a local regulation of this phosphatase. Although NFAT has not been reported to be part of a macromolecular complex organized by AKAPs, there is some evidence that this transcription factor also resides in distinct cytosolic domains and that its regulation occurs locally.[47] Based on the above observations, a possible scenario is therefore that PDE2 controls a pool of cAMP that activates an AKAP-bound PKA type II

to phosphorylate a local NFAT, possibly counterbalancing its dephosphorylation by a local Ca^{2+}-calmodulin–dependent phosphatase. Further studies are required to explore this hypothesis.

Recently, it has been reported by Mehel et al[48] that norepinephrine treatment does not significantly increase cell size in ARVM-overexpressing PDE2. Based on this observation, the authors suggest that PDE2 may be protective against pathological hypertrophy. Unfortunately, that report showed only normalized values of the effect of norepinephrine on cells overexpressing PDE2 and not the effect on cell size of overexpression of PDE2 per se, making the data difficult to interpret. We note, however, that although the authors draw the opposite conclusion, the data as reported by Mehel et al are compatible with the findings described in the present report. If we were to express the effect of norepinephrine on cell size relative to control cells and relative to PDE2 overexpressing cells, as reported in the Mehel et al study, the latter group would show a significantly blunted effect of norepinephrine treatment (see Online Figure XII and refer to Online Figures IIIA, IIIB, VIIE, and VIIF). However, this way of presenting the data is misleading because overexpression of PDE2 already results in significant hypertrophy compared with control cells and, thus, reduces the relative effect of norepinephrine (see Figure 3 and Online Figure III).

Our findings may have important clinical implications. The in vivo data indicate that inhibition of PDE2 counteracts hypertrophy in a TAC model. Additional investigations will be required to establish whether this would protect against progression toward heart failure and to determine the relevance of PDE2 activity to human cardiac hypertrophy. Increased PDE2 expression has been reported in early rat cardiac hypertrophy,[49] as well as in failing human hearts,[50] suggesting that increased activity of this enzyme may be involved in the pathogenesis of the disease. It has been suggested that the hypertrophic response to pathological stress is never truly adaptive[51] and that inhibition of hypertrophy is beneficial.[52–54] In addition, the possibility to control the local concentration of cAMP at specific sites via selective inhibition of PDEs has been previously recognized as a possible approach to improving clinical outcomes,[55] and a phase 3 trial has been recently concluded where the PDE3-selective inhibitor enoximone was used in combination with β-blockade to couple inhibition of adverse β-adrenergic signaling with restoration of phospholamban phosphorylation.[56] From this perspective, PDE2 may represent a particularly interesting target. In vitro studies have demonstrated that the pool of cAMP generated on inhibition of PDE2 mediates positive inotropic effects,[18,57] and the ability to manipulate a pool of cAMP that simultaneously exerts positive inotropy and counteracts cardiac myocyte hypertrophic growth may represent a significant improvement over existing therapeutic strategies.

Sources of Funding

This study was supported by the Fondation Leducq (O6 CVD 02), the British Heart Foundation (BHF; PG/10/75/28537 and RG/12/3/29423) to M. Zaccolo and the BHF Oxford Centre of Research Excellence grant (RE/13/1/30181) to K. Lefkimmiatis; the Fondation Leducq (O6 CVD 02), American Heart Association (10034439), and US Department of Veterans Affairs (CARA-029-09F) grants to M. Movsesian; and the Research Counsel of Norway and KG Jebsen Cardiac Research Center to I. Sjaastad and J.M. Aronsen.

Disclosures

None.

References

1. El-Armouche A, Eschenhagen T. Beta-adrenergic stimulation and myocardial function in the failing heart. *Heart Fail Rev*. 2009;14:225–241. doi: 10.1007/s10741-008-9132-8.
2. Zaccolo M, Pozzan T. Discrete microdomains with high concentration of cAMP in stimulated rat neonatal cardiac myocytes. *Science*. 2002;295:1711–1715. doi: 10.1126/science.1069982.
3. Nikolaev VO, Moshkov A, Lyon AR, Miragoli M, Novak P, Paur H, Lohse MJ, Korchev YE, Harding SE, Gorelik J. Beta2-adrenergic receptor redistribution in heart failure changes cAMP compartmentation. *Science*. 2010;327:1653–1657. doi: 10.1126/science.1185988.
4. Hayes JS, Brunton LL, Brown JH, Reese JB, Mayer SE. Hormonally specific expression of cardiac protein kinase activity. *Proc Natl Acad Sci U S A*. 1979;76:1570–1574.
5. Hayes JS, Brunton LL. Functional compartments in cyclic nucleotide action. *J Cyclic Nucleotide Res*. 1982;8:1–16.
6. Di Benedetto G, Zoccarato A, Lissandron V, Terrin A, Li X, Houslay MD, Baillie GS, Zaccolo M. Protein kinase A type I and type II define distinct intracellular signaling compartments. *Circ Res*. 2008;103:836–844. doi: 10.1161/CIRCRESAHA.108.174813.
7. Scott JD, Santana LF. A-kinase anchoring proteins: getting to the heart of the matter. *Circulation*. 2010;121:1264–1271. doi: 10.1161/CIRCULATIONAHA.109.896357.
8. Carr DW, Stofko-Hahn RE, Fraser ID, Bishop SM, Acott TS, Brennan RG, Scott JD. Interaction of the regulatory subunit (RII) of cAMP-dependent protein kinase with RII-anchoring proteins occurs through an amphipathic helix binding motif. *J Biol Chem*. 1991;266:14188–14192.
9. Hulme JT, Westenbroek RE, Scheuer T, Catterall WA. Phosphorylation of serine 1928 in the distal C-terminal domain of cardiac CaV1.2 channels during beta1-adrenergic regulation. *Proc Natl Acad Sci U S A*. 2006;103:16574–16579. doi: 10.1073/pnas.0607294103.
10. Lygren B, Carlson CR, Santamaria K, Lissandron V, McSorley T, Litzenberg J, Lorenz D, Wiesner B, Rosenthal W, Zaccolo M, Taskén K, Klussmann E. AKAP complex regulates Ca2+ re-uptake into heart sarcoplasmic reticulum. *EMBO Rep*. 2007;8:1061–1067. doi: 10.1038/sj.embor.7401081.
11. Marx SO, Kurokawa J, Reiken S, Motoike H, D'Armiento J, Marks AR, Kass RS. Requirement of a macromolecular signaling complex for beta adrenergic receptor modulation of the KCNQ1-KCNE1 potassium channel. *Science*. 2002;295:496–499. doi: 10.1126/science.1066843.
12. Gold MG, Lygren B, Dokurno P, Hoshi N, McConnachie G, Taskén K, Carlson CR, Scott JD, Barford D. Molecular basis of AKAP specificity for PKA regulatory subunits. *Mol Cell*. 2006;24:383–395. doi: 10.1016/j.molcel.2006.09.006.
13. Banky P, Newlon MG, Roy M, Garrod S, Taylor SS, Jennings PA. Isoform-specific differences between the type Ialpha and IIalpha cyclic AMP-dependent protein kinase anchoring domains revealed by solution NMR. *J Biol Chem*. 2000;275:35146–35152. doi: 10.1074/jbc.M003961200.
14. Maurice DH, Ke H, Ahmad F, Wang Y, Chung J, Manganiello VC. Advances in targeting cyclic nucleotide phosphodiesterases. *Nat Rev Drug Discov*. 2014;13:290–314. doi: 10.1038/nrd4228.
15. Leroy J, Abi-Gerges A, Nikolaev VO, Richter W, Lechêne P, Mazet JL, Conti M, Fischmeister R, Vandecasteele G. Spatiotemporal dynamics of beta-adrenergic cAMP signals and L-type Ca2+ channel regulation in adult rat ventricular myocytes: role of phosphodiesterases. *Circ Res*. 2008;102:1091–1100. doi: 10.1161/CIRCRESAHA.107.167817.
16. Stangherlin A, Gesellchen F, Zoccarato A, Terrin A, Fields LA, Berrera M, Surdo NC, Craig MA, Smith G, Hamilton G, Zaccolo M. cGMP signals modulate cAMP levels in a compartment-specific manner to regulate catecholamine-dependent signaling in cardiac myocytes. *Circ Res*. 2011;108:929–939. doi: 10.1161/CIRCRESAHA.110.230698.

17. Mongillo M, McSorley T, Evellin S, Sood A, Lissandron V, Terrin A, Huston E, Hannawacker A, Lohse MJ, Pozzan T, Houslay MD, Zaccolo M. Fluorescence resonance energy transfer-based analysis of cAMP dynamics in live neonatal rat cardiac myocytes reveals distinct functions of compartmentalized phosphodiesterases. *Circ Res*. 2004;95:67–75. doi: 10.1161/01.RES.0000134629.84732.11.
18. Mongillo M, Tocchetti CG, Terrin A, Lissandron V, Cheung YF, Dostmann WR, Pozzan T, Kass DA, Paolocci N, Houslay MD, Zaccolo M. Compartmentalized phosphodiesterase-2 activity blunts beta-adrenergic cardiac inotropy via an NO/cGMP-dependent pathway. *Circ Res*. 2006;98:226–234. doi: 10.1161/01.RES.0000200178.34179.93.
19. Haworth RS, Cuello F, Avkiran M. Regulation by phosphodiesterase isoforms of protein kinase A-mediated attenuation of myocardial protein kinase D activation. *Basic Res Cardiol*. 2011;106:51–63. doi: 10.1007/s00395-010-0116-1.
20. Nichols CB, Chang CW, Ferrero M, Wood BM, Stein ML, Ferguson AJ, Ha D, Rigor RR, Bossuyt S, Bossuyt J. β-adrenergic signaling inhibits Gq-dependent protein kinase D activation by preventing protein kinase D translocation. *Circ Res*. 2014;114:1398–1409. doi: 10.1161/CIRCRESAHA.114.303870.
21. Mudd JO, Kass DA. Tackling heart failure in the twenty-first century. *Nature*. 2008;451:919–928. doi: 10.1038/nature06798.
22. White DC, Hata JA, Shah AS, Glower DD, Lefkowitz RJ, Koch WJ. Preservation of myocardial beta-adrenergic receptor signaling delays the development of heart failure after myocardial infarction. *Proc Natl Acad Sci U S A*. 2000;97:5428–5433. doi: 10.1073/pnas.090091197.
23. Lai NC, Roth DM, Gao MH, Fine S, Head BP, Zhu J, McKirnan MD, Kwong C, Dalton N, Urasawa K, Roth DA, Hammond HK. Intracoronary delivery of adenovirus encoding adenylyl cyclase VI increases left ventricular function and cAMP-generating capacity. *Circulation*. 2000;102:2396–2401.
24. Sucharov CC, Dockstader K, Nunley K, McKinsey TA, Bristow M. β-Adrenergic receptor stimulation and activation of protein kinase A protect against α1-adrenergic-mediated phosphorylation of protein kinase D and histone deacetylase 5. *J Card Fail*. 2011;17:592–600. doi: 10.1016/j.cardfail.2011.03.006.
25. Simpson P. Stimulation of hypertrophy of cultured neonatal rat heart cells through an alpha 1-adrenergic receptor and induction of beating through an alpha 1- and beta 1-adrenergic receptor interaction. Evidence for independent regulation of growth and beating. *Circ Res*. 1985;56:884–894.
26. Martins TJ, Mumby MC, Beavo JA. Purification and characterization of a cyclic GMP-stimulated cyclic nucleotide phosphodiesterase from bovine tissues. *J Biol Chem*. 1982;257:1973–1979.
27. Nickl CK, Raidas SK, Zhao H, Sausbier M, Ruth P, Tegge W, Brayden JE, Dostmann WR. (D)-Amino acid analogues of DT-2 as highly selective and superior inhibitors of cGMP-dependent protein kinase Ialpha. *Biochim Biophys Acta*. 2010;1804:524–532. doi: 10.1016/j.bbapap.2009.12.004.
28. Takimoto E, Champion HC, Li M, Belardi D, Ren S, Rodriguez ER, Bedja D, Gabrielson KL, Wang Y, Kass DA. Chronic inhibition of cyclic GMP phosphodiesterase 5A prevents and reverses cardiac hypertrophy. *Nat Med*. 2005;11:214–222. doi: 10.1038/nm1175.
29. Hodges RR, Zoukhri D, Sergheraert C, Zieske JD, Dartt DA. Identification of vasoactive intestinal peptide receptor subtypes in the lacrimal gland and their signal-transducing components. *Invest Ophthalmol Vis Sci*. 1997;38:610–619.
30. Carr DW, Hausken ZE, Fraser ID, Stofko-Hahn RE, Scott JD. Association of the type II cAMP-dependent protein kinase with a human thyroid RII-anchoring protein. Cloning and characterization of the RII-binding domain. *J Biol Chem*. 1992;267:13376–13382.
31. McCahill A, McSorley T, Huston E, Hill EV, Lynch MJ, Gall I, Keryer G, Lygren B, Tasken K, van Heeke G, Houslay MD. In resting COS1 cells a dominant negative approach shows that specific, anchored PDE4 cAMP phosphodiesterase isoforms gate the activation, by basal cyclic AMP production, of AKAP-tethered protein kinase A type II located in the centrosomal region. *Cell Signal*. 2005;17:1158–1173. doi: 10.1016/j.cellsig.2005.04.003.
32. Terrin A, Monterisi S, Stangherlin A, Zoccarato A, Koschinski A, Surdo NC, Mongillo M, Sawa A, Jordanides NE, Mountford JC, Zaccolo M. PKA and PDE4D3 anchoring to AKAP9 provides distinct regulation of cAMP signals at the centrosome. *J Cell Biol*. 2012;198:607–621. doi: 10.1083/jcb.201201059.
33. Carlson CR, Lygren B, Berge T, Hoshi N, Wong W, Taskén K, Scott JD. Delineation of type I protein kinase A-selective signaling events using an RI anchoring disruptor. *J Biol Chem*. 2006;281:21535–21545. doi: 10.1074/jbc.M603223200.
34. Molkentin JD, Lu JR, Antos CL, Markham B, Richardson J, Robbins J, Grant SR, Olson EN. A calcineurin-dependent transcriptional pathway for cardiac hypertrophy. *Cell*. 1998;93:215–228.
35. Beals CR, Sheridan CM, Turck CW, Gardner P, Crabtree GR. Nuclear export of NF-ATc enhanced by glycogen synthase kinase-3. *Science*. 1997;275:1930–1934.
36. Sheridan CM, Heist EK, Beals CR, Crabtree GR, Gardner P. Protein kinase A negatively modulates the nuclear accumulation of NF-ATc1 by priming for subsequent phosphorylation by glycogen synthase kinase-3. *J Biol Chem*. 2002;277:48664–48676. doi: 10.1074/jbc.M207029200.
37. Vega RB, Rothermel BA, Weinheimer CJ, Kovacs A, Naseem RH, Bassel-Duby R, Williams RS, Olson EN. Dual roles of modulatory calcineurin-interacting protein 1 in cardiac hypertrophy. *Proc Natl Acad Sci U S A*. 2003;100:669–674. doi: 10.1073/pnas.0237225100.
38. Wilkins BJ, Dai YS, Bueno OF, Parsons SA, Xu J, Plank DM, Jones F, Kimball TR, Molkentin JD. Calcineurin/NFAT coupling participates in pathological, but not physiological, cardiac hypertrophy. *Circ Res*. 2004;94:110–118. doi: 10.1161/01.RES.0000109415.17511.18.
39. Asakura M, Kitakaze M, Takashima S, et al. Cardiac hypertrophy is inhibited by antagonism of ADAM12 processing of HB-EGF: metalloproteinase inhibitors as a new therapy. *Nat Med*. 2002;8:35–40. doi: 10.1038/nm0102-35.
40. Zhang X, Szeto C, Gao E, et al. Cardiotoxic and cardioprotective features of chronic β-adrenergic signaling. *Circ Res*. 2013;112:498–509. doi: 10.1161/CIRCRESAHA.112.273896.
41. Enns LC, Bible KL, Emond MJ, Ladiges WC. Mice lacking the Cβ subunit of PKA are resistant to angiotensin II-induced cardiac hypertrophy and dysfunction. *BMC Res Notes*. 2010;3:307. doi: 10.1186/1756-0500-3-307.
42. Ha CH, Kim JY, Zhao J, Wang W, Jhun BS, Wong C, Jin ZG. PKA phosphorylates histone deacetylase 5 and prevents its nuclear export, leading to the inhibition of gene transcription and cardiomyocyte hypertrophy. *Proc Natl Acad Sci U S A*. 2010;107:15467–15472. doi: 10.1073/pnas.1000462107.
43. Abrenica B, AlShaaban M, Czubryt MP. The A-kinase anchor protein AKAP121 is a negative regulator of cardiomyocyte hypertrophy. *J Mol Cell Cardiol*. 2009;46:674–681.
44. Nichols CB, Rossow CF, Navedo MF, Westenbroek RE, Catterall WA, Santana LF, McKnight GS. Sympathetic stimulation of adult cardiomyocytes requires association of AKAP5 with a subpopulation of L-type calcium channels. *Circ Res*. 2010;107:747–756. doi: 10.1161/CIRCRESAHA.109.216127.
45. Li J, Negro A, Lopez J, Bauman AL, Henson E, Dodge-Kafka K, Kapiloff MS. The mAKAPbeta scaffold regulates cardiac myocyte hypertrophy via recruitment of activated calcineurin. *J Mol Cell Cardiol*. 2010;48:387–394. doi: 10.1016/j.yjmcc.2009.10.023.
46. Makarewich CA, Correll RN, Gao H, Zhang H, Yang B, Berretta RM, Rizzo V, Molkentin JD, Houser SR. A caveolae-targeted L-type Ca^{2}+ channel antagonist inhibits hypertrophic signaling without reducing cardiac contractility. *Circ Res*. 2012;110:669–674. doi: 10.1161/CIRCRESAHA.111.264028.
47. Rinne A, Kapur N, Molkentin JD, Pogwizd SM, Bers DM, Banach K, Blatter LA. Isoform- and tissue-specific regulation of the Ca(2+)-sensitive transcription factor NFAT in cardiac myocytes and heart failure. *Am J Physiol Heart Circ Physiol*. 2010;298:H2001–H2009. doi: 10.1152/ajpheart.01072.2009.
48. Mehel H, Emons J, Vettel C, et al. Phosphodiesterase-2 is up-regulated in human failing hearts and blunts β-adrenergic responses in cardiomyocytes. *J Am Coll Cardiol*. 2013;62:1596–1606. doi: 10.1016/j.jacc.2013.05.057.
49. Hua R, Adamczyk A, Robbins C, Ray G, Rose RA. Distinct patterns of constitutive phosphodiesterase activity in mouse sinoatrial node and atrial myocardium. *PLoS One*. 2012;7:e47652. doi: 10.1371/journal.pone.0047652.
50. Aye TT, Soni S, van Veen TA, van der Heyden MA, Cappadona S, Varro A, de Weger RA, de Jonge N, Vos MA, Heck AJ, Scholten A. Reorganized PKA-AKAP associations in the failing human heart. *J Mol Cell Cardiol*. 2012;52:511–518. doi: 10.1016/j.yjmcc.2011.06.003.
51. Perrino C, Naga Prasad SV, Mao L, Noma T, Yan Z, Kim HS, Smithies O, Rockman HA. Intermittent pressure overload triggers hypertrophy-independent cardiac dysfunction and vascular rarefaction. *J Clin Invest*. 2006;116:1547–1560. doi: 10.1172/JCI25397.
52. Frey N, Katus HA, Olson EN, Hill JA. Hypertrophy of the heart: a new therapeutic target? *Circulation*. 2004;109:1580–1589. doi: 10.1161/01.CIR.0000120390.68287.BB.

53. Esposito G, Rapacciuolo A, Naga Prasad SV, Takaoka H, Thomas SA, Koch WJ, Rockman HA. Genetic alterations that inhibit in vivo pressure-overload hypertrophy prevent cardiac dysfunction despite increased wall stress. *Circulation*. 2002;105:85–92.
54. Koitabashi N, Kass DA. Reverse remodeling in heart failure–mechanisms and therapeutic opportunities. *Nat Rev Cardiol*. 2012;9:147–157. doi: 10.1038/nrcardio.2011.172.
55. Bristow MR. Treatment of chronic heart failure with β-adrenergic receptor antagonists: a convergence of receptor pharmacology and clinical cardiology. *Circ Res*. 2011;109:1176–1194. doi: 10.1161/CIRCRESAHA.111.245092.
56. Metra M, Eichhorn E, Abraham WT, et al; ESSENTIAL Investigators. Effects of low-dose oral enoximone administration on mortality, morbidity, and exercise capacity in patients with advanced heart failure: the randomized, double-blind, placebo-controlled, parallel group ESSENTIAL trials. *Eur Heart J*. 2009;30:3015–3026. doi: 10.1093/eurheartj/ehp338.
57. Gesztelyi R, Zsuga J, Hajdú P, Szabó JZ, Cseppento A, Szentmiklósi AJ. Positive inotropic effect of the inhibition of cyclic GMP-stimulated 3′,5′-cyclic nucleotide phosphodiesterase (PDE2) on guinea pig left atria in eu- and hyperthyroidism. *Gen Physiol Biophys*. 2003;22:501–513.

Novelty and Significance

What Is Known?

- 3′-5′-Cyclic adenosine monophosphate (cAMP)/protein kinase A (PKA) signals are critical regulators of heart function in health and disease.
- Phosphodiesterases (PDEs), the enzymes that degrade cAMP, modulate the local activity of cAMP/PKA, resulting in compartmentalized signaling.
- Different PDE isoenzymes regulate spatially distinct pools of cAMP, but the role of these individual local cAMP pools in the pathogenesis of heart disease is unclear.

What New Information Does This Article Contribute?

- Distinct pools of cAMP affect cardiac myocyte hypertrophic growth differently.
- Inhibition of PDE3 and PDE4 results in cardiac hypertrophy, whereas inhibition of PDE2 is antihypertrophic.
- The antihypertrophic effect of PDE2 inhibition relies on a local increase in cAMP and PKA-mediated phosphorylation of the nuclear factor of activated T cells.

cAMP/PKA signaling controls cardiac function, and its downregulation is involved in the pathophysiology of cardiac hypertrophy, an early feature of cardiac remodeling leading to heart failure. Therapeutic intervention aimed at sustaining contractility by raising cAMP levels, although effective in the short term, is associated with increased mortality in the long term. The rationale of our study was based on the hypothesis that different pools of cAMP may have either positive or negative effects on cardiac function and that available treatments targeting the cAMP pathway fail to selectively affect those pools of cAMP involved in sustaining contractility and have a predominant negative effect by promoting cardiac remodeling. Here we investigate the effects of selectively inhibiting individual PDE isoforms on cardiac hypertrophy. We find that although inhibition of PDE3 or PDE4 is prohypertrophic, inhibition of PDE2 mediates antihypertrophic effects. We demonstrate that the antihypertrophic effect of PDE2 inhibition involves the generation of a local pool of cAMP and activation of a subset of PKA type II that phosphorylates the prohypertrophic transcription factor nuclear factor of activated T cells, blocking its nuclear translocation. Our findings demonstrate, for the first time, the involvement of PDE2 in the development of cardiac hypertrophy and identify PDE2 as a potential novel therapeutic target to treat this condition.

Circulation Research
JOURNAL OF THE AMERICAN HEART ASSOCIATION

Cardiac Hypertrophy Is Inhibited by a Local Pool of cAMP Regulated by Phosphodiesterase 2

Anna Zoccarato, Nicoletta C. Surdo, Jan M. Aronsen, Laura A. Fields, Luisa Mancuso, Giuliano Dodoni, Alessandra Stangherlin, Craig Livie, He Jiang, Yuan Yan Sin, Frank Gesellchen, Anna Terrin, George S. Baillie, Stuart A. Nicklin, Delyth Graham, Nicolas Szabo-Fresnais, Judith Krall, Fabrice Vandeput, Matthew Movsesian, Leonardo Furlan, Veronica Corsetti, Graham Hamilton, Konstantinos Lefkimmiatis, Ivar Sjaastad and Manuela Zaccolo

Circ Res. 2015;117:707-719; originally published online August 4, 2015;
doi: 10.1161/CIRCRESAHA.114.305892
Circulation Research is published by the American Heart Association, 7272 Greenville Avenue, Dallas, TX 75231

Print ISSN: 0009-7330. Online ISSN: 1524-4571

Supplemental Material

Materials and Methods

Reagents. Norepinephrine, cilostamide, rolipram, and forskolin were from Sigma-Aldrich. BAY 60-7550 was from Alexis. Collagenase A was from Roche, Pancreatin from Sigma, Laminin (mouse) from BD Biosciences. Phosphate-Buffered Saline (PBS), DMEM High Glucose, MEM199, Horse Serum, New born Calf Serum, Penicilline/Streptomycine (10,000 units of penicillin (base) and 10,000 µg of streptomycin (base)/mL) and Glutamine were from Invitrogen. Sildenafil was a kind gift from Sharron Francis, Vanderbilt University School of Medicine, Nashville, Tennessee. DT-2 was from BioLog and myrPKI from Calbiochem. BIO was purchased from EMD Biosciences and SP6000125 was from Calbiochem. Antibody against GFP was purchased from Abcam and was used according to the manufacturer's instructions. Anti-phospho-RXXS/T antibody was from Cell Signaling.

Mouse models. All animal procedures in this study were carried out according to the Home Office regulations regarding experiments with animals in the UK, the European Community guiding principles for the care and the 'Regulations on Animal Experimentation' under The Norwegian Animal Welfare Act and approved by the Norwegian Animal Research Authority (FDU application 7105) and use of animals and the projects were approved by the local ethic committees. Male C57Bl/6 mice were from Charles River. Pressure overload was produced by TAC as described in[1]. Briefly, thoracotomy was performed in the second intercostal space, the transverse aorta between right and left carotid arteries was isolated and a 7-0 nylon suture ligature was placed around the aorta, with the two ends of the suture left outside the chest. Hemodynamic recording was continuously acquired under basal conditions and during a 5 s acute transverse aortic occlusion produced by gently pulling on the suture ends. The suture ligature was tied against a 27 G needle, which was rapidly removed to result in a significant pressure load on the LV. The chest was closed and mice were allowed to recover. Sham- operated mice underwent the same operation, but without aortic constriction. Treatment with PDE2 inhibitor (BAY 60-7550, 3 mg/kg) or vehicle (sunflower oil) was provided by intraperitoneal injection, three times a day.
In a subset of the TAC mice echocardiography was performed 24h after the TAC-procedure with a Vevo2100 system (FUJIFILM VisualSonics Inc, Toronto, Canada) to obtain the maximal flow velocity over the TAC. Stratification was performed by assessing the flow velocity over the TAC, before randomization to either treatment with PDE2 inhibitor (BAY 60-7550, 3 mg/kg x 3 per day with intraperitoneal injection for 21 days) or corresponding vehicle (sunflower oil).
In a separate set of experiments, cardiac specific NFAT-reporter mice [2] (kindly donated by Professor Jeffrey Molkentin, Department of Pediatrics, Cincinnati Children's Hospital Medical Center, University of Cincinnati, US) with nine copies of an NFAT-binding site from the interleukin-4 promoter inserted upstream of the luciferase gene underwent the same procedure and were treated with PDE2 inhibitor over 14 days to measure the role of PDE2 inhibition on NFAT-activity in hypertrophic hearts.
3 weeks after surgical procedure, pressure was measured under anaesthesia as systolic pressure gradient between left and right carotid arteries using a high-fidelity micromanometer catheter (Millar Instruments). Immediately following, the mice were weighed then the hearts were excised and the ratio of left ventricular weight to body weight (LVW/BW) was calculated.

Echocardiography, magnetic resonance imaging and cardiac phenotyping. Left ventricular mass was estimated with cardiac MRI (CMRI), echocardiography and measured post mortem at the end of the protocol. CMRI was performed on a 9.4T preclinical MR system (Agilent Technologies, Inc., CA) with high-performance gradient (60 mm ID, rise time 180 µs, max strength 100 gauss/cm) and a quadrature volume RF coils (35 mm ID, Rapid

Biomedical, Washington, USA) as previously described [3]. Mice were sedated and mask ventilated with a mixture of O_2 and 1.0-1.5% isoflurane during the protocol, and body temperature was maintained by heated air guided by continuous body temperature recording during the protocol. CMRI cine loops were acquired with ECG-triggering and respiration gating using a motion compensated gradient echo sequence. Apical to basal left ventricular short-axis slices (8-10) were acquired with echo-/repetition time=2.1/4.6 ms; field-of-view =25.6x25.6 mm; acquisition matrix 128x128; slice thickness =1.0 mm; flip angle 15°; averages =2. Mass estimates were obtained both in systole and diastole, and <5% variance was accepted.
Left ventricular mass was calculated with the following formula from echocardiography: (IVSd + LVDd + PWDd)^3 – LVDd^3, where LVDd is the left ventricle diameter in diastole and IVSd/PWDd is the interventricular septum and posterior wall thickness in diastole, respectively. After final echocardiography, left ventricular (LV) mass was measured by cardiac excision in deep surgical anesthesia and rapid dissection of the LV chamber, which was weighed and frozen in liquid nitrogen for further analysis.

Histology. Paraffin-embedded left ventricles were cut into 5 µm slices. Sections were stained with Picrosirius red (Fluka, Buchs, Switzerland) as described[1]. Cross-sectional areas were measured using the ImageJ software (National Institutes of Health). Appropriate cross-sections were defined as those showing nearly circular capillary profiles and nuclei.

NRVMs culture, treatment and transfection. Primary cultured cardiac ventricular myocytes were isolated from 1 to 2-days old Sprague-Dawley rats (Charles River Laboratories Wilmington, MA) as previously described[4]. Cells were cultured in 1st day medium (DMEM High Glucose, MEM199, Horse serum, New born Calf serum, Glutamine, Pen/Strep) for 24 hours before switching to a serum-free medium containing DMEM High Glucose, MEM199, Insulin-Transferring-Selenium-X Supplement, Glutamine, Pen/Strep. After 24 hours cells were treated for 48 hours with norepinephrine (10 µmol/L) and/or other stimuli, as indicated. NRVMs were transfected with Transfectin Lipid Reagent (BioRAD), following the supplier's instructions. NFATC1-GFP was a kind gift from Stefano Schiaffino, University of Padova. NFATC1-GFP triple mutant was generated by introducing the S245A, S269A and S294A mutations by site directed mutagenesis using standard molecular biology techniques.

ARVMs culture, treatment and adenoviral delivery. Wistar rats aged 16 weeks were sacrificed by cervical dislocation. Single cardiomyocytes were isolated as previously described[5]. Briefly, hearts were rapidly removed, cannulated, perfused and digested with 0.6 mg mL-1 collagenase type I (Worthington) and 0.04 mg mL-1 protease type XIV (Sigma). Isolated cardiomyocytes were resuspended in MEM199 medium supplemented with 5 mmol/L creatine (Sigma), 5 mmol/L taurine (Sigma), 2 mmol/L carnitine (Sigma), 1% Pen/Strep and plated on laminin-coated 24 mm coverslips. After 2 hours undigested tissue and unattached cells were washed off and the remaining cardiomyocytes were treated with different stimuli and/or transduced with AdV5/PDE2A wild type or AdV5/PDE2A D685A-D796A (at 100 PFU/cell) for 24h.

Adenoviral vector generation. PDE2A wild type and PDE2A D685A-D796A were cloned into the pShuttle-CMV vector and transferred by homologous recombination into the pAdEasy-1 vector and then transfected into 293 cells to generate AdV5/CMV/PDE2A wild type and AdV5/CMV/PDE2A D685A-D796A (using AdEasy™ XL Adenoviral Vector System from Agilent Technologies - Stratagene Products). For *in vivo* experiments AdV5-PDE2A wild type-mCherry and AdV5-PDE2A D685A-D796A-mCherry produced by Vector Biolabs were purified and titrated using standard techniques[6].

Intracardiac injection of AdV5-PDE2A mcherry. *In vivo* experiments were performed in 20-24 week old Wistar Kyoto (WKY) male rats according to the Home Office regulations

regarding experiments with animals in the UK. Briefly, the animal underwent isofluorane anesthesia (2.5%) and endotracheal intubation. Under sterile conditions, left thoracotomy was performed in the fourth intercostal space, the left lung collapsed and the pericardium opened. Direct intramyocardial injection of the apical region of the exposed heart was carried out using 5 injections of 50 µL volume for a titre of $5x10^8$ pfu recombinant adenovirus (AdV5-PDE2A wild type mCherry or AdV5-PDE2A D685A-D796A-mCherry) in a total volume of 250 µL in sterile PBS using a 29 G needle. Lungs were re-inflated and the chest was rapidly closed. The animal was given post-operative analgesia (buprenorphine (0.05 mg/kg) and carprofen (5 mg/kg) and closely monitored until full recovery from anaesthesia. 7 days after injection the rat was sacrificed by cervical dislocation, and single cardiac myocytes were isolated and cell surface area measured in both transduced (mCherry positive) and untransduced cells.

Real-time PCR. Total RNA was extracted from cultured NRVMs using RNeasy® Mini Kit (Qiagen) and reverse transcription of RNA samples was carried out by using QuantiTect® Reverse Transcription Kit (Qiagen) according to manufacturer's instructions. For PDE2, the TaqMan® Gene Expression Assay Rn00579346_m1 from Applied Biosystems was utilised. 18S rRNA Primers and TaqMan probe sequences; Forward: 5'-CGCGGTTCTATTTTGTTGGT-3', Reverse: 5'-CGGTCCAAGAATTTCACCTC-3', TaqMan: 5'-FAM-TGAGGCCATGATTAAGAGGG-TAM-3'. Real-time PCR reactions were prepared using Platinum® Quantitative PCR SuperMix UDG with ROX (Invitrogen) and performed in a 7300 Real time PCR System (Applied Biosystems). For quantification of BNP and RCAN1, frozen left ventricular samples were homogenised using the Precellys tissue homogeniser (2 times for 20 sec), total RNA was extracted using aRNeasy Fibrous Tissue Mini Kit (Qiagen) and reverse transcription of RNA samples was carried out by using QuantiTect® Reverse Transcription Kit (Qiagen) according to manufacturer's instructions. The primer sequences used for GAPDH are the following; Forward: ATGACAACTTTGTCAAGCTCATTT, Reverse: GGTCCACCACCCTGTTGCT. For BNP; Forward: AAGGGAGAATACGGCATCATTG, Reverse: ACAGCACCTTCAGGAGATCCA. For RCAN1.4; Forward: CCCGTGAAAAAGCAGAATGC, Reverse: TCCTTGTCATATGTTCTGAAGAGGG.

PDE2 knock down. Knock down of PDE2A was achieved using a siGENOME SMARTpool siRNA (125 nmol/L) (M-094898-00-0020, Rat PDE2A, NM_031079, Thermo scientific) as previously described[5]. Rescue of PDE2 was performed by co-transfection of a plasmid containing PDE2Awt-mRFP and a siRNA sequence designed to target the 3′-untranslated region (UTR) of PDE2 (5'-GCAGAAGGAATTCGAGATT-3', Thermo Scientific), a region that is not present in the plasmid sequence. Control experiments were carried out using siGLO Red transfection indicator (125 nmol/L) according to manufacturer's instructions (D-001630-02-20, Thermo scientific).

Cell size and NFAT-GFP nuclear translocation measurements. Images of single adult or neonatal rat ventricular myocytes were taken in brightfield mode on an Olympus IX71 inverted microscope, Olympus PlanApoN objective, NA 1.42 oil, 0.17/FN 26.5, and Meta imaging series 7.1, MetaMorph, (Molecular Devices). When required, epifluorescence microscopy images were taken using either YFP illumination set (excitation filter ET500/30x, dichroic mirror T515LP, emission filter ET535/30m, Chroma Technology) or an RFP set (TxRed-A-Basic-000, single band excitation filter FF01-559/34-25, dichroic mirror FF585-Di01-25x36, single band emitter FF01-630/69-25, Semrock) Cell surface area was calculated by drawing a region of interest (ROI) including the cell and by counting the number of pixels within the ROI. One pixel corresponds to 0.1075 µm when images are collected with 60x objective (experiments with NRVMs), or to 0.1613 µm when images are acquired with 40x objective (ARVMs experiments). For NFAT-GFP experiments, cells scored as positive for NFAT-GFP nuclear translocation were those showing a GFP fluorescent signal in the nucleus at least as high as the fluorescent signal in the cytosol.

[^{3}H] Leucine incorporation assay. 24 h after serum starvation NRVMs were incubated with 10 µmol/L NE in the presence or absence of Bay 60-7550 (10 µmol/L) for 36 h. NRVMs were then incubated in the same medium with 1.0 µCi/ml [^{3}H] Leucine for an additional 12 h. The medium was then washed off the cells with ice-cold PBS and cells were fixed on ice for 30 min with cold 10% TCA. After washing twice with 10% TCA and once with water, the radioactivity incorporated into the TCA precipitate was determined by liquid scintillation counting after solubilisation in 0.1 M NaOH for 10 minutes.

FRET imaging. FRET imaging experiments were performed 24-48 h after NRVMs transfection with the Epac1-camps FRET sensor[7]. Cells were maintained at room temperature in a Ringer modified saline (NaCl 125 mmol/L, KCl 5 mmol/L, Na_3PO_4 1 mmol/L, $MgSO_4$ 1 mmol/L, Hepes 20 mmol/L, Glucose 5.5 mmol/L, $CaCl_2$ 1 mmol/L, pH 7.4), and imaged on an inverted microscope (Olympus IX71) using a PlanApoN, 60X, NA 1.42 oil immersion objective, 0.17/FN 26.5 (Olympus, UK). The microscope was equipped with a coolSNAP HQ monochrome camera system (Photometrics) and a beam-splitter optical device (Dual-view simultaneous-imaging system, DV2 mag biosystem, Photometrics, ET-04-EM). The FRET filter settings used throughout were: CFP excitation filter ET436/20x, dichroic mirror 455DCLP (Chroma Technology) in the microscope filter cube; dichroic mirror 505DCLP, YFP emission filter 545 nm, and CFP emission filter 480 nm (Chroma Technology) in the beam splitter. Images were acquired and processed using Meta imaging series 7.1, MetaFluor, (Molecular Devices). FRET changes were measured as changes in the background-subtracted 480/545 nm fluorescence emission intensity on excitation at 430 nm and expressed as R/R_0, where R is the ratio at time t and R_0 is the ratio at time = 0 s. Value are expressed as mean ± SEM.

Pull downs, Immunoprecipitation and Western Blot. For pull down experiments, Neonatal Rat Ventricular Myocytes (NRVMs) were transfected with equal amounts of NFAT-GFP together with a plasmid expressing the potent PKA inhibitor protein Protein Kinase inhibitor (PKI) isoform alpha tagged with mCherry or, as control, same quantity of a plasmid expressing only the tag (mCherry). Twenty-four hours after transfection, cells were treated with NE (10µM) or NE plus Bay60-7550 (10µM) for 10 minutes. Cells were lysed using RIPA buffer (Sigma) complemented with protease and phosphatase inhibitor cocktail (Thermo Scientific). Insoluble material was removed by centrifugation at 14,000g for 10 min at 4oC and total protein was quantified by the Bradford method (Sigma). For the pull down experiments cell lysates were incubated for 2h-4h at 4^{o}C with 25µl of agarose beads coated with a monoclonal anti-GFP antibody (Chromotek). Beads were washed five times with ice-cold PBS and the proteins were released with 25µl of 2x SDS-loading buffer. For the immunoprecipitation experiments, 6x 10^6 NRVMs were plated into 10cm petri dishes coated with laminin. The day after cells were rinsed twice with ADS buffer and their medium replaced with serum free media. Cells were treated for 48h with NE (10µM), BAY60-7550 (10µM), Rolipram (10µM) alone or their combinations. For mouse left ventricles whole cell lysates from frozen tissue were obtained by homogenisation in lysis buffer (CelLytic™ MT, C3228; Sigma) with protease (Complete Mini EDTA-free tablets; Roche Diagnostics) and phosphatase inhibitors PhosSTOP Phosphatase Inhibitor Cocktail Tablet; Roche Diagnostics) using Precellys tissue homogeniser (2 times for 20 sec). Protein concentrations were determined by Micro BCA Protein Assay Kit (Pierce, Rockford, IL).1mg-2mg of total cell or tissue lysates were pre-cleared rotating for 2h at 4^{o}C with 25-50µl of agarose beads. After pre-clearing 2µg of anti-NFAT mouse monoclonal antibody (or normal mouse Igg for the control) were added to the samples and were allowed to incubate ON at 4 ^{o}C. The day after 20µl of agarose beads (G) were added and allowed to incubate for additional 2-4h at 4 ^{o}C. Afterwards beads were washed five times with ice-cold PBS and finally re-suspended with 25µl of 2x SDS-loading buffer. Pulled down or immunoprecipitated proteins were released from the beads at 95^{o}C for 5 min and then were resolved on 5%-20% tris-acetate SDS/PAGE gels (Life sciences) and electro-blotted

onto PVDF membranes (Hybond-P, Amersham Biosciences, Piscataway, NJ). After transfer PVDF membranes were blocked for 1h at room temperature in 5% milk with Tris-buffered saline/Tween 20 (TBST; 10mM Tris HCl, PH 8.0/150mM NaCl/0.1% Tween 20). The membranes were incubated over night at 4 ^{o}C with the primary antibodies. After five washes with TBST, membranes were incubated at room temperature for 2h with appropriate peroxidase-conjugated secondary antibodies. Peroxidase activity was detected with chemiluminescence (ECL western blotting detection kit, Thermo Scientific). Glyceraldehyde-3-phosphate dehydrogenase (GAPDH) antibody (1:2000; Santa Cruz) was used as a loading control for the total cell lysates and to detect protein contamination for the immunoprecipitated proteins, while anti-GFP or anti NFAT antibodies were used to control for efficient pull down and immunoprecipitation respectively. For the experiment shown in Suppl. Fig. 9, after preclearing, proteins were immunoprecipitated overnight at 4^{o}C with anti-GFP antibody and the immunocomplexes were retrieved using Protein A beads (Invitrogen). The immunoprecipitates were then collected by centrifugation at 13'000 rpm for 3 min and washed three times with lysis buffer. Bound proteins were then eluted in SDS-PAGE sample buffer and subjected to SDS-PAGE and immunoblotting for phospho-RXXS/T. The blots were stripped with stripping buffer (Thermo Scientific) and reprobed with anti-GFP antibody as internal controls. For the experiments shown in Fig. 7A and B, proteins were immunoprecipitated with anti phospho-PKA substrate (Cell Signalling) and the immunoblots were performed with anti-GFP antibody (Santa Cruz). Control experiments were performed using normal rabbit IgG (Santa Cruz). Quantification of the band intensity was accomplished by densitometry using Quantity One 1-D software (Bio-Rad).

Luciferase assay. NFAT activation was followed by reporter assays using adenoviral transduction of NFAT reporter vector Ad-NFAT-Luc (Vector Biolabs). Infection efficiency of the adenoviral vectors was controlled by fluorescence microscopy using the mCherry expressing adenoviral vector Ad-mCherry (Vector Biolabs) and calculated at 90%-95%. Freshly isolated NRVMs were counted and equal amounts of cells were seeded in 6-well plates, pre-coated with laminin. The day after platting cells were washed with ADS and the media replaced with serum free medium. Cells were treated with Phenylephrine (PE) or left untreated. The next day cell media was complemented with the GSK-3 kinase inhibitor 6-bromoindirubin-3'-oxime (BIO) (5µM) or the JNK kinase inhibitor SP6000125 (SP6) (20µM) (Calbiochem). Twenty-four hours after cells were lysed and luciferase expression was determined by using the Dual-Luciferase Reporter Assay system (Promega Corporation, WI, USA).
Luciferase activity in heart tissue from NFAT-reporter mice was measured with the Luciferase Assay System protocol (E1000, Promega) according to the manufacturer's protocol. Left ventricular myocardium was homogenized and mixed with the substrate buffer after normalizing for protein concentration in each homogenate. Luminescence was measured with a Victor3 1420 Multilabel Counter (PerkinElmer, Waltham, MA) and normalized to sham values. Four repeats were performed per heart, where each repeat was normalized to corresponding sham values.

Statistical analysis. Data were expressed as mean ± s.e.m. Differences between multiple groups were compared by analysis of variance (ANOVA) followed by a Tukey's or Dunnett's multiple comparisons tests. Two-group analysis was performed by *t*-test. Number of replicates is indicated in the figure legends. *p≤0.05; **p≤ 0.01; *** p ≤ 0.005; ns= not significant.

Online Table I

	TAC + vehicle	TAC + BAY 60-7550
TAC pressure gradient (m/s)	3.2±0.1	3.2±0.1
Left atrial diameter (LAD) (mm)	2.1±0.1	2.0±0.1
Left ventricle diameter (LVDd) (mm)	4.1±0.2	4.1±0.1

Baseline data calculated from echocardiography recordings after randomization to BAY 60 7550 or vehicle in C57/Bl6 mice obtained at day 1 after TAC surgery. $p>0.4$

Online Table II

	TAC + vehicle	TAC + BAY 60-7550
TAC pressure gradient (m/s)	3.2±0.1	2.9±0.1
Left atrial diameter (LAD) (mm)	1.8±0.04	1.9±0.1
Left ventricle diameter (LVDd) (mm)	3.3±0.1	3.2±0.2

Baseline data calculated from echocardiography recordings after randomization to BAY 60 7550 or vehicle in NFAT reporter mice obtained at day 1 after TAC surgery. $p>0.1$

Online Figure I

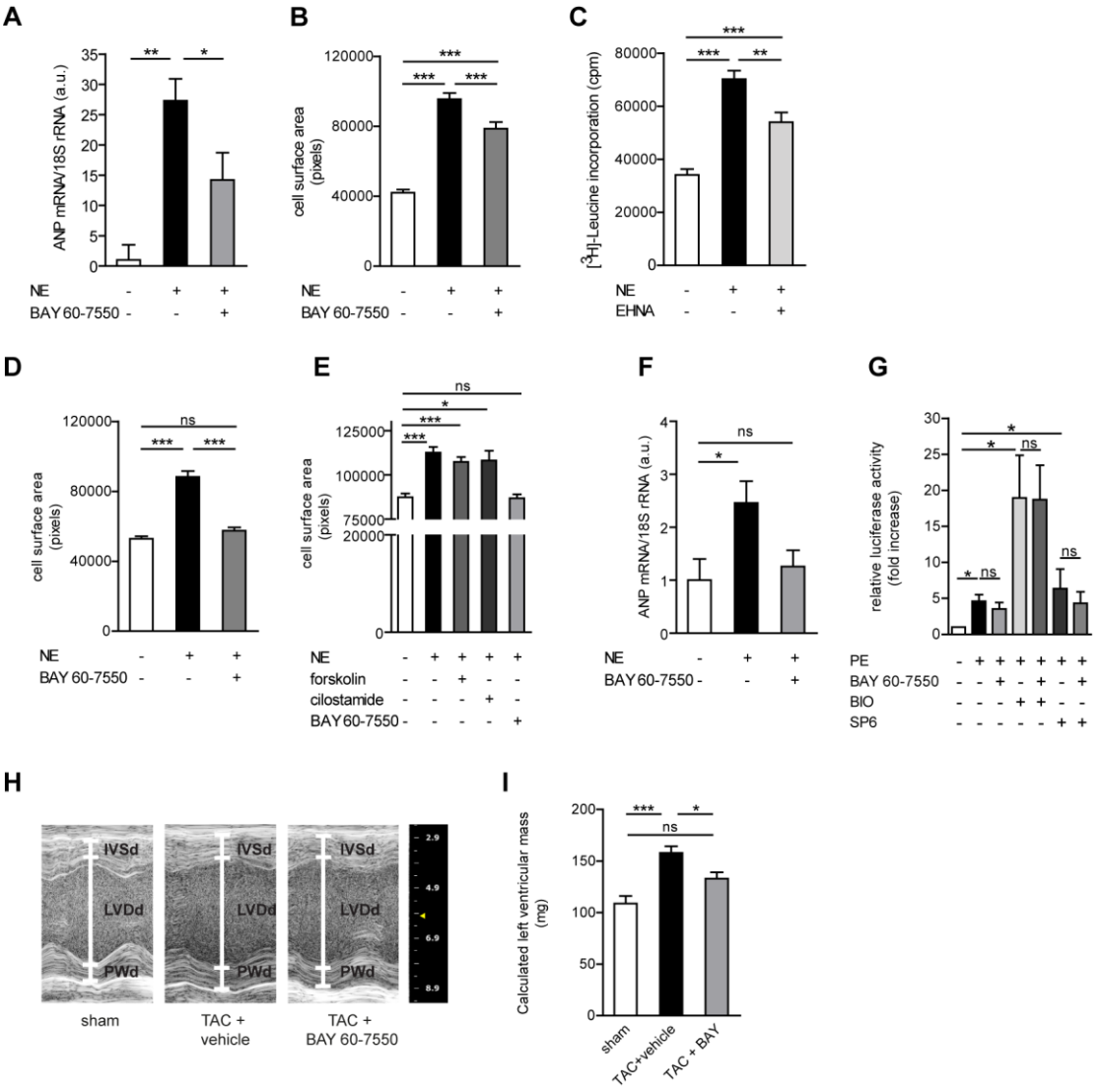

Online Figure I. (A) ANP mRNA levels (mean ± s.e.m of 3 independent experiments) measured in NRVMs treated for 48 hours with NE (10 µmol/L), or with NE (10 µmol/L) + BAY 60-7550 (10µmol/L) as indicated. **(B)** Cell surface area measured for control or NRVMs treated with NE (10 µmol/L), or with NE (10 µmol/L) + BAY 60-7550 (50 nmol/L) (mean ± s.e.m of a minimum of n=71 cells per condition). **(C)** [^{3}H] leucine incorporation (mean ± s.e.m of n ≥ 27 independent experiments) measured in NRVMs untreated or treated with NE (10 µmol/L) or NE plus EHNA (10 µmol/L). **(D)** Cell size measured for cardiac myocytes isolated from neonatal mice and treated for 48 hours with NE (10 µmol/L) alone or in combination with BAY 60-7550 (10 µmol/L) as indicated (mean ± s.e.m of a minimum of n=113 cells per condition). Pixel size= 0.1075 µm. **(E)** Cell surface area of ARVMs untreated or treated for 24 hours with NE (1 µmol/L), or NE in combination with forskolin (1 µmol/L), cilostamide (10 µmol/L), or BAY 60-7550 (50 nmol/L) (mean ± s.e.m of a minimum of n=17 cells per condition). Pixel size= 0.1613 µm**. (F)** ANP mRNA levels (mean ± s.e.m of a minimum of 9 independent experiments) measured for ARVMs untreated or treated with NE (1 µmol/L) or NE plus BAY 60-7550 (50 nmol/L). **(G)** Luciferase activity relative measured in NRVMs treated for 48 hours with PE (10 µmol/L), BAY 60-7550 (10 µmol/L), BIO (5 µmol/L) and SP6

(20 µmol/L)as indicated (mean ± s.e.m of 5 independent experiments). **(H)** Representative long axis echocardiographic M-mode recordings of left ventricle in C57/Bl6 TAC mice treated as indicated for 3 weeks. **(I)** Left ventricular mass calculated by echocardiography in C57/Bl6 TAC mice after 3 weeks with BAY 60-7550 or vehicle treatment (n=4-6 mice per group). One -way ANOVA and Tukey's multiple comparison tests were utilized in all data set. * $p \leq 0.05$; ** $p \leq 0.01$; *** $p \leq 0.005$; ns= not significant.

Online Figure II

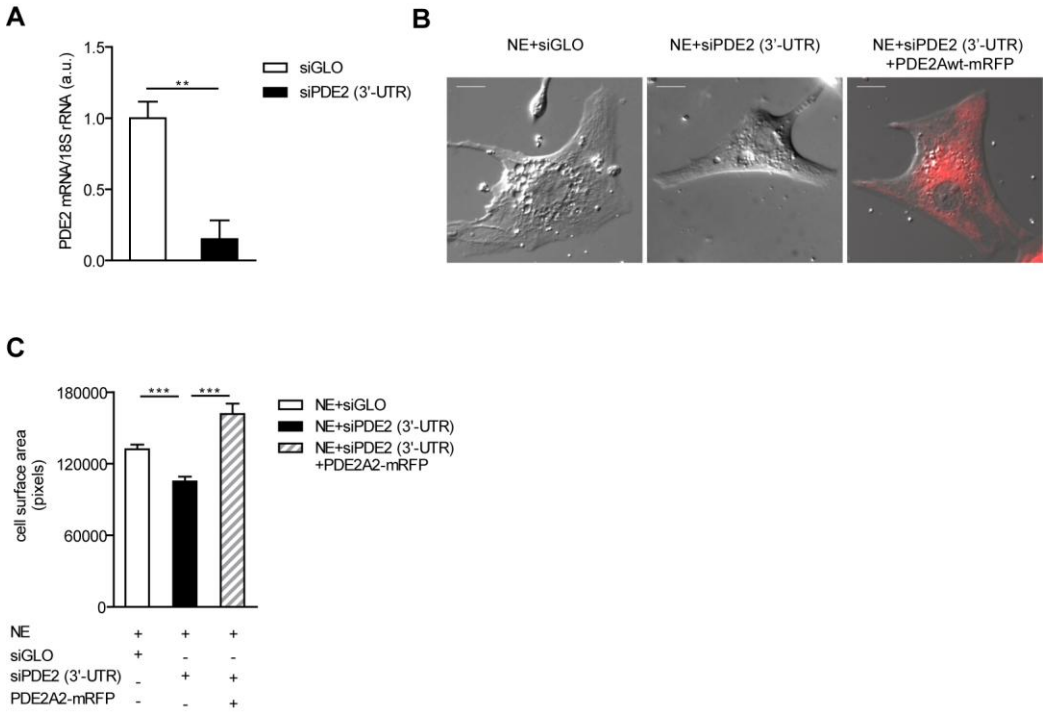

Online Figure II (A) PDE2 mRNA levels in cell expressing the control siGLO Red or siPDE2 (3'-UTR) sequences and measured by RT-PCR. **(B)** Representative DIC images of NE-treated NRVMs expressing siGLO Red (left panel), siPDE2 (3'-UTR) (middle panel) or siPDE2 (3'-UTR) in combination with siRNA-resistant PDE2Awt-mRFP (right panel). The panel on the right also show, as an overlay with the DIC image, the fluorescence signal from PDE2Awt-mRFP. Scale bar: 10 µm. **(C)** Summary of cell surface area calculated for NRVMs treated with NE and transfected with siGLO Red, or siPDE2 (3'-UTR), or siPDE2 (3'-UTR) and PDE2A-mRFP (mean± s.e.m of 3 independent experiments, number of cells ≥56). *t*-test was performed in A and One-way ANOVA and Tukey's multiple comparison test in C. Pixel size= 0.1075 µm. ** p ≤0,01; *** p≤ 0,005.

Online Figure III

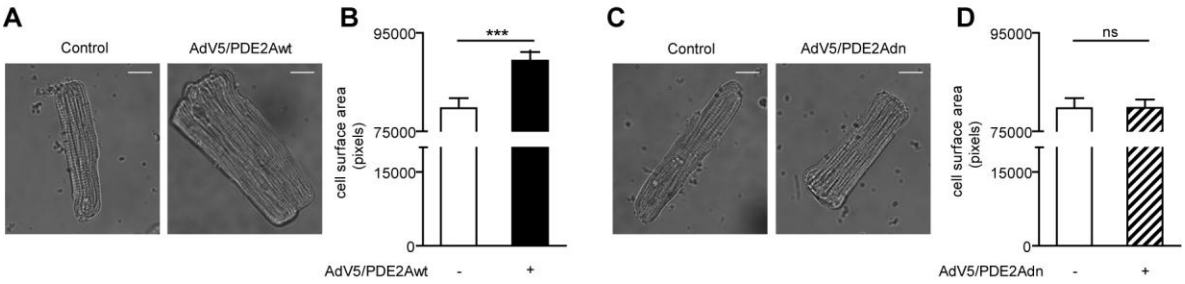

Online Figure III. (A) Image of representative cells and **(B)** cell surface area measured for control ARVMs and ARVMs transduced *in vitro* with AdV5/PDE2Awt at 100 plaque forming unit (PFU)/cell. **(C)** Representative cells and **(D)** cell surface area calculated for untransduced ARVMs or ARVMs infected with AdV5/PDE2Adn (mean± s.e.m of 3 independent experiments, number of cells ≥100). Pixel size = 0.1613 µm. Scale bar: 10 µm. *t*-test was utilised for statistical analysis. *** p≤ 0,005; ns= not significant.

Online Figure IV

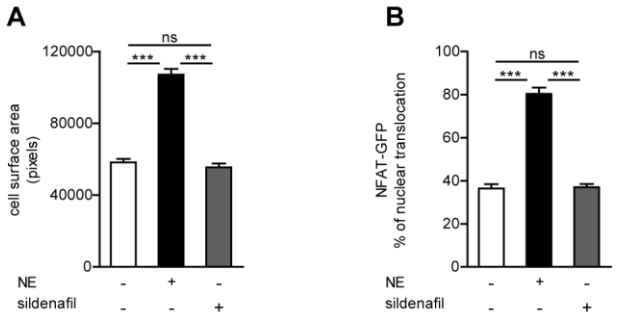

Online Figure IV. Cell size **(A)** and NFAT-GFP nulcear translocation **(B)** calculated for control, NRVMs treated with NE (10 µmol/L) or with the selective PDE5 inhibitor sildenafil (10 nmol/L) (mean ± s.e.m of n ≥ 85 cells per conditions and of n =4 independent experiments respectively). One-way ANOVA and Tukey's multiple comparison tests were performed. *** p≤0.005; ns= not significant.

Online Figure V

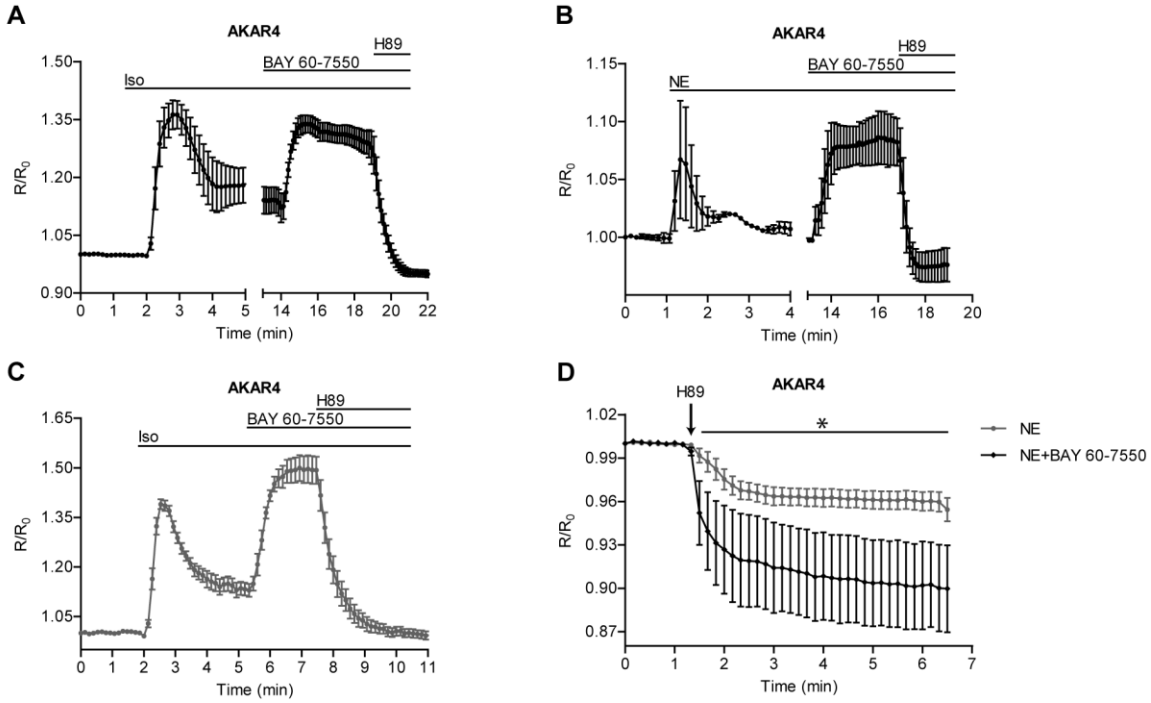

Online Figure V. (A) Normalized mean kinetics of FRET change induced by isoproterenol (10nmol/L), BAY 60-7550 (10µmol/L) and H89 (10µmol/L) in NRVMs expressing the cytosolic PKA activity reporter AKAR4[8]. **(B)** Normalized mean kinetics of FRET change induced by NE (10nmol/L), BAY 60-7550 (10µmol/L) and H89 (10µmol/L) in NRVMs expressing AKAR4. **(C)** Normalized mean kinetics measured in hypertrophied NRVMs (treated for 48 hours with 10µmol/L NE) expressing AKAR4 and challenged with isoproterenol (10nmol/L), BAY 60-7550 (10µmol/L) and H89 (10µmol/L). **(D)** Normalized mean kinetics of FRET change induced by H89 (10µmol/L) in NRVMs expressing the cytosolic PKA activity reporter AKAR4 and treated for 48 hours with NE (10µmol/L) or NE plus BAY 60-7550 (10µmol/L). n≥4; *t*-test was performed in D. * p≤0.05

Online Figure VI

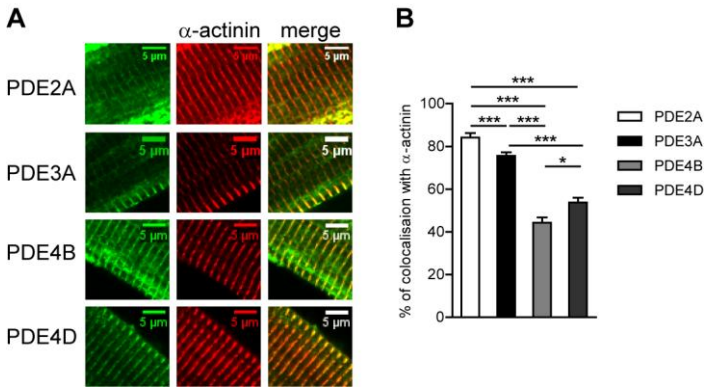

Online Figure VI. To gain insight on the different subcellular localisation of individual PDEs we have performed immunostaining using family specific antibodies to PDEs and assessed the overlay of their signal with α-actinin immunostaining used as a reference for the sarcomeric Z line. We have used the Pearson's correlation coefficient to estimate the degree of colocalisation of different PDEs with the Z line and taken a significant difference in this parameter as an indication of different localisation of PDEs. **(A)** Representative images of ARVMs co-stained with specific antibodies against PDE2A, PDE3A, PDE4B or PDE4D and anti-α-actinin antibody. **(B)** Co-localisation of PDE staining and α-actinin was measured as Pearson's correlation coefficient. One-way ANOVA and Tukey's multiple comparison tests were utilised. *** $p \leq 0.005$; * $p \leq 0.05$.

Online Figure VII

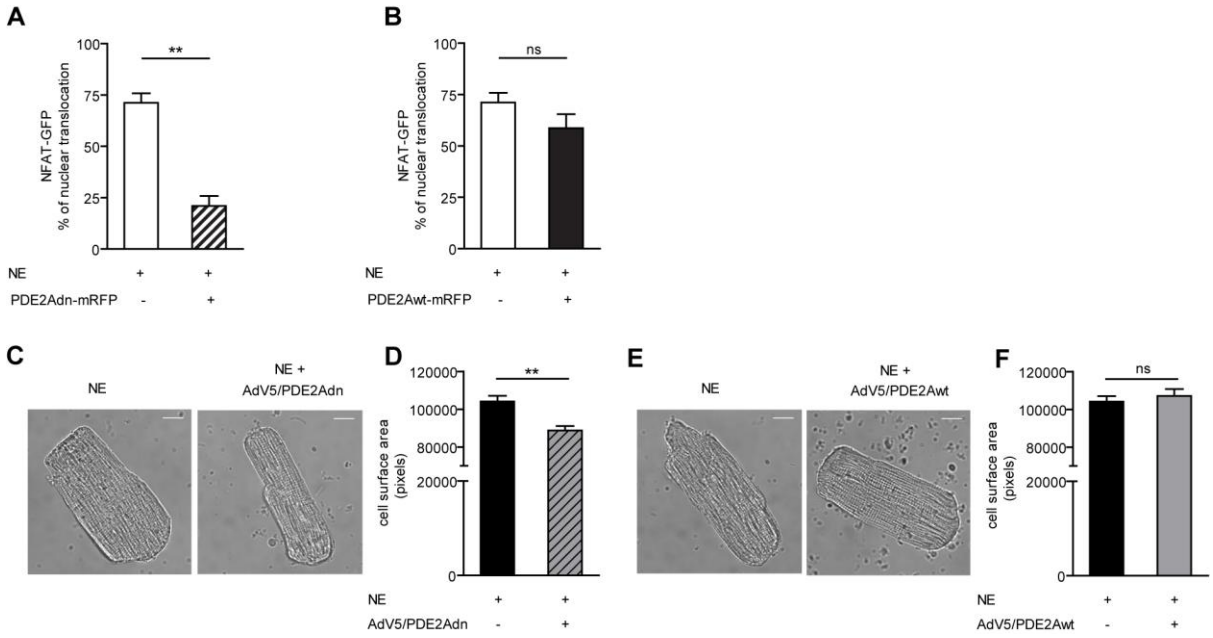

Online Figure VII. (A) Percentage of cells showing NFAT-nuclear translocation (mean± s.e.m of 3 independent experiments, number of cells ≥51) for NE-treated myocytes or NE-treated myocytes expressing PDE2Adn-mRFP. **(B)** NFAT-nuclear translocation measurements (mean± s.e.m of 3 independent experiments, number of cells ≥58) for NE-treated NRVMs and NRVMs treated with NE and overexpressing PDE2Awt-mRFP. **(C)** Images of representative cells and **(D)** cell surface area of NE-treated ARVMs in the absence or presence of overexpressed PDE2Adn (mean± s.e.m of 3 independent experiments, number of cells ≥68). **(E)** Representative images and **(F)** cell surface area of NE-treated ARVMs in the absence or presence of overexpressed PDE2Awt (mean± s.e.m of 3 independent experiments, number of cells ≥68). Pixel size = 0.1613 µm. Scale bar: 10 µm. For all experiments a *t*-test statistical analysis was performed. ** p ≤0.01; ns= not significant.

Online Figure VIII

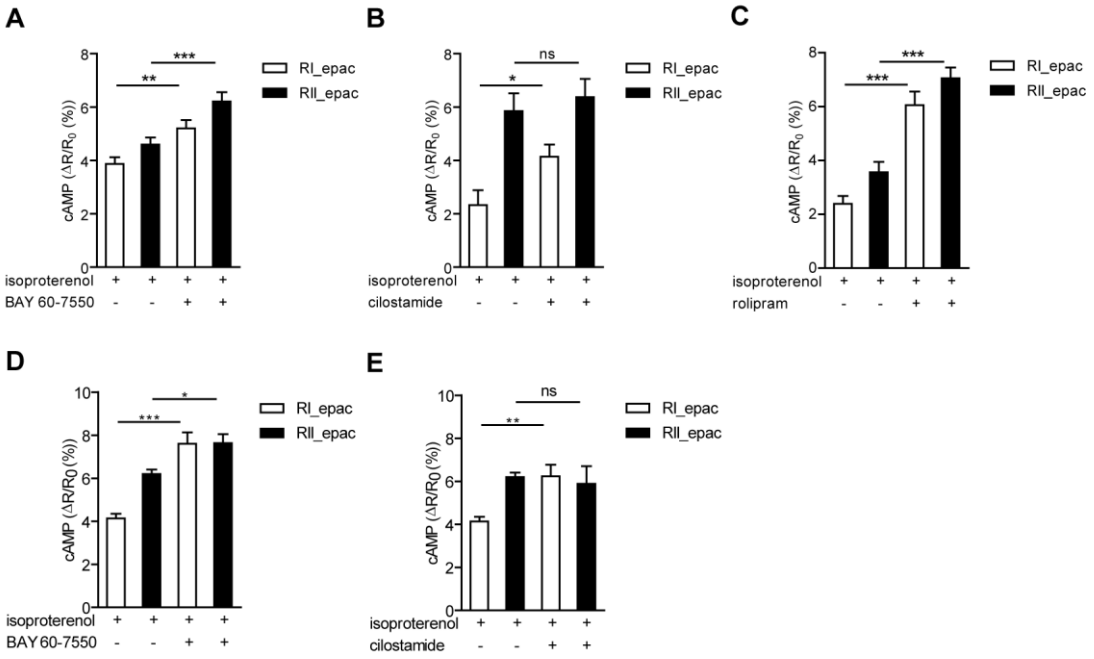

Online Figure VIII. cAMP changes detected in NRVMs by RI-epac (white bars) or by RII-epac (black bars) upon stimulation with 10 nmol/L isoproterenol followed by addition of either 10 µM BAY 60-7550 **(A),** or of 10 µmol/L cilostamide **(B)** or rolipram **(C)**; data are mean ± s.e.m, n≥9 cells. cAMP changes induced by 10 nmol/L isoproterenol followed by either 10 µmol/L BAY 60-7550 **(D)** or of 10 µmol/L cilostamide **(E)** in ARVMs expressing RI-epac or RII-epac; data are mean ± s.e.m, n≥8 cells. For all experiments a *t*-test statistical analysis was performed. *** p≤ 0.005; ** p ≤0.01; * p ≤ 0.05; ns= not significant.

Online Figure IX

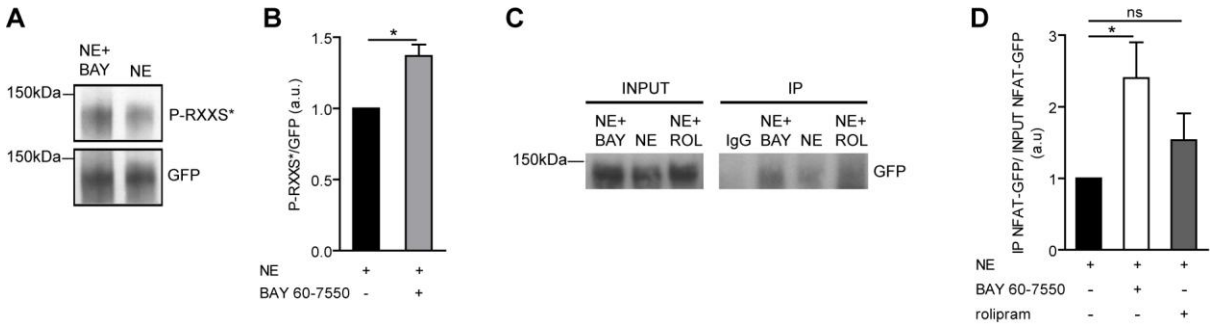

Online Figure IX. (A) Representative western blot of NFAT-GFP pull down from NRVMs treated with NE or NE and BAY 60-7550 and probed with a PKA substrate antibody (upper panel, P-RXXS* signal) and with a GFP-specific antibody (lower panel). **(B)** Quantification of the experiment shown in (A). **(C)** Representative image and **(D)** quantification of 4 independent pull down experiments performed using an anti Phospho-PKA substrate antibody on lysates from NRVMs expressing NFAT-GFP, treated with NE, NE plus BAY 60-7550 or NE plus rolipram (10 µmol/L) and probed with a GFP-specific antibody Values are mean± s.e.m of 3 independent experiments.

Online Figure X

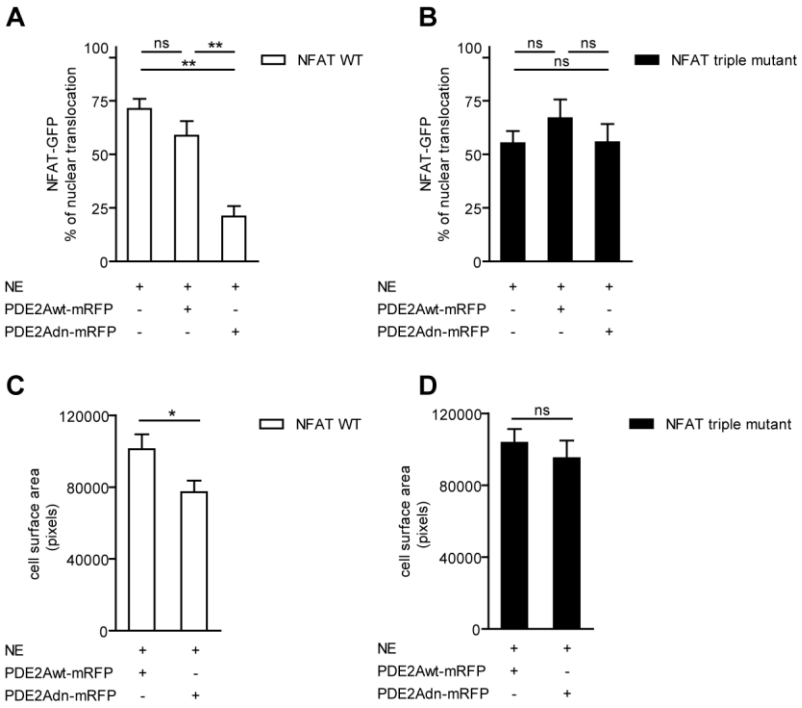

Online Figure X. (A) Nuclear translocation of NFAT-GFP for NRVMs treated with NE and overexpressing PDE2Awt-mRFP or PDE2Adn-mRFP as indicated (3 independent experiments, n ≥51). **(B)** Nuclear translocation of NFAT-GFP triple mutant calculated for NRVMs treated with NE and overexpressing PDE2Awt-mRFP or PDE2Adn-mRFP (3 independent experiments, n≥48). **(C)** Summary of cell surface area for NE-treated NRVMs expressing NFAT-GFP wild type and PDE2Awt-mRFP or PDE2Adn-mRFP as indicated (3 independent experiments, n ≥35). **(D)** Cell surface area of NE-treated NRVMs expressing NFAT-GFP triple mutant and PDE2Awt-mRFP or PDE2Adn-mRFP as indicated (3 independent experiments, n ≥20). In C and D *t*-test was utilised, one-way ANOVA and Tukey's multiple comparison tests were performed in A and B. Pixel size= 0.1075 µm. * p ≤ 0.05; ** p ≤0.01; ns= not significant.

Online Figure XI

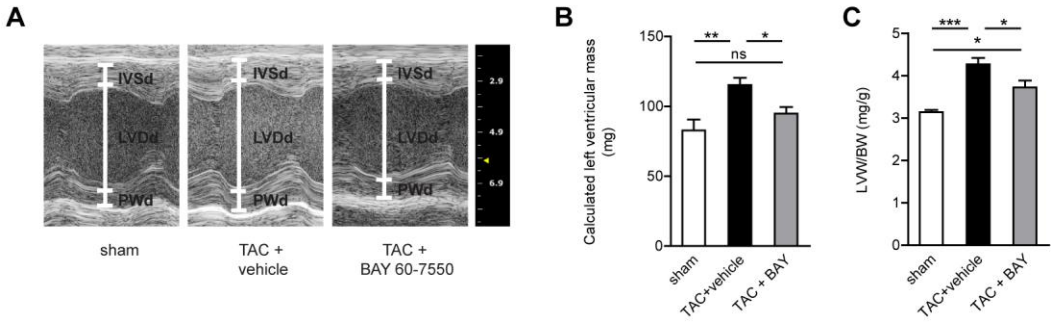

Online Figure XI. (A) Representative long axis echocardiographic M-mode recordings of left ventricle from NFAT reporter TAC mice treated as indicated for 2 weeks. **(B)** Left ventricular mass calculated by echocardiography in NFAT reporter TAC mice after 2 weeks treatment with BAY 60-7550 or vehicle. **(C)** LVW/BW ratio values calculated post-mortem in NFAT reporter TAC mice after 2 weeks with BAY 60-7550 or vehicle treatment as indicated. One-way ANOVA and Tukey's multiple comparison tests were performed n=5-8 mice per group. * $p \leq 0.05$; ** $p \leq 0.01$; *** $p \leq 0.001$; ns= not significant.

Online Figure XII

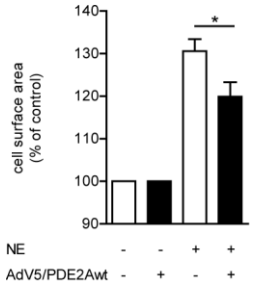

Online Figure XII. ARVMs were stimulated with 10 µmol/L NE for 24 h and infected with adenovirus encoding for PDE2A wild type (AdV5/PDE2). Cell surface area of NE treated cells is expressed as percentage of their relative untreated controls (100%) as in Mehel et al[9]. *t*-test statistical analysis was performed. * $p \leq 0.05$

References

1. Patrucco E, Notte A, Barberis L, Selvetella G, Maffei A, Brancaccio M, Marengo S, Russo G, Azzolino O, Rybalkin SD, Silengo L, Altruda F, Wetzker R, Wymann MP, Lembo G, Hirsch E. Pi3kgamma modulates the cardiac response to chronic pressure overload by distinct kinase-dependent and -independent effects. *Cell*. 2004;118:375-387
2. Wilkins BJ, Dai YS, Bueno OF, Parsons SA, Xu J, Plank DM, Jones F, Kimball TR, Molkentin JD. Calcineurin/nfat coupling participates in pathological, but not physiological, cardiac hypertrophy. *Circulation research*. 2004;94:110-118
3. Espe EK, Aronsen JM, Eriksen GS, Zhang L, Smiseth OA, Edvardsen T, Sjaastad I, Eriksen M. Assessment of regional myocardial work in rats. *Circulation. Cardiovascular imaging*. 2015;8:e002695
4. Zaccolo M, Pozzan T. Discrete microdomains with high concentration of camp in stimulated rat neonatal cardiac myocytes. *Science*. 2002;295:1711-1715
5. Stangherlin A, Gesellchen F, Zoccarato A, Terrin A, Fields LA, Berrera M, Surdo NC, Craig MA, Smith G, Hamilton G, Zaccolo M. Cgmp signals modulate camp levels in a compartment-specific manner to regulate catecholamine-dependent signaling in cardiac myocytes. *Circ Res*. 2011
6. Alba R, Baker AH, Nicklin SA. Vector systems for prenatal gene therapy: Principles of adenovirus design and production. *Methods Mol Biol*. 2012;891:55-84
7. Nikolaev VO, Bunemann M, Hein L, Hannawacker A, Lohse MJ. Novel single chain camp sensors for receptor-induced signal propagation. *J. Biol. Chem.* 2004;279:37215-37218
8. Depry C, Allen MD, Zhang J. Visualization of pka activity in plasma membrane microdomains. *Molecular bioSystems*. 2011;7:52-58
9. Mehel H, Emons J, Vettel C, Wittkopper K, Seppelt D, Dewenter M, Lutz S, Sossalla S, Maier LS, Lechene P, Leroy J, Lefebvre F, Varin A, Eschenhagen T, Nattel S, Dobrev D, Zimmermann WH, Nikolaev VO, Vandecasteele G, Fischmeister R, El-Armouche A. Phosphodiesterase-2 is up-regulated in human failing hearts and blunts beta-adrenergic responses in cardiomyocytes. *Journal of the American College of Cardiology*. 2013;62:1596-1606